THE ASTRONOMICAL JOURNAL, 118:488–508, 1999 July

A *HUBBLE SPACE TELESCOPE* SURVEY FOR RESOLVED COMPANIONS OF PLANETARY NEBULA NUCLEI

ROBIN CIARDULLO,[1] HOWARD E. BOND,[2] MICHAEL S. SIPIOR,[1] LAURA K. FULLTON,[2,3]
C.-Y. ZHANG,[2,4] AND KAREN G. SCHAEFER[2,5]
Received 1999 March 1; accepted 1999 April 7

ABSTRACT

We report the results of a *Hubble Space Telescope*[6] "snapshot" survey aimed at finding resolved binary companions of the central stars of Galactic planetary nebulae (PNe). Using the the Wide Field and Planetary Camera and Wide Field Planetary Camera 2, we searched the fields of 113 PNe for stars whose close proximity to the central star suggests a physical association. In all, we find 10 binary nuclei that are very likely to be physically associated and another six that are possible binary associations. By correcting for interstellar extinction and placing the central stars' companions on the main sequence (or, in one case, on the white dwarf cooling curve), we derive distances to the objects, and thereby significantly increase the number of PNe with reliable distances. Comparison of our derived distances with those obtained from various statistical methods shows that all of the latter have systematically overestimated the distances, by factors ranging up to a factor of 2 or more. We show that this error is most likely due to the fact that the properties of our PNe with binary nuclei are systematically different from those of PNe used heretofore to calibrate statistical methods. Specifically, our PNe tend to have lower surface brightnesses at the same physical radius than the traditional calibration objects. This difference may arise from a selection effect: the PNe in our survey are typically nearby, old nebulae, whereas most of the objects that calibrate statistical techniques are low-latitude, high surface brightness, and more distant nebulae. As a result, the statistical methods that seem to work well with samples of distant PNe, for example, those in the Galactic bulge or external galaxies, may not be applicable to the more diverse population of local PNe. Our distance determinations could be improved with better knowledge of the metallicities of the individual nebulae and central stars, measurements of proper motions and radial velocities for additional candidate companions, and deeper *HST* images of several of our new binary nuclei.

Key words: planetary nebulae: general — binaries: visual — stars: distances — stars: AGB and post-AGB

1. INTRODUCTION

Planetary nebulae (PNe) are extraordinarily useful for probing stellar evolution and cosmology. In extragalactic astronomy, the planetary nebula luminosity function (PNLF) is one of the most accurate and reliable indicators of relative distance (see the review of Jacoby et al. 1992); in stellar astrophysics, PNe allow us to examine the physics of mass loss and the timescales of stellar evolution (e.g., the review of Iben 1995). Since young PNe are bright emission-line sources, they make ideal test particles for dynamical studies, both in the Milky Way and in external galaxies (e.g., Ciardullo, Jacoby, & Dejonghe 1993; Amaral et al. 1996). Finally, since the chemical abundances in a PN reflect the chemistry of the interstellar medium (ISM) at the time of its progenitor's formation (with some light species possibly altered subsequently by stellar nucleosynthesis), these objects can yield unique insights into galactic star formation histories and chemical and stellar evolution (cf. Dopita et al. 1997).

Almost every interesting quantity related to PNe in the Milky Way—their space density, formation rate, Galactic distribution, sizes, ionized and total nebular masses, contribution to chemical evolution, and the luminosities and evolutionary states of their central stars—depends critically upon their distances. But, unfortunately, the distances to PNe within the Galaxy are known only poorly. It is a remarkable irony that while the PNLF can be used to derive relative distances to external galaxies to better than $\sim 10\%$ (cf. Jacoby et al. 1992), the distances to Milky Way PNe are typically known to no better than a factor of ~ 2 or worse (e.g., Terzian 1993, 1997). In fact, of the ~ 1100 known Galactic PNe, only a dozen or so have distances that are reasonably well determined using direct methods. For the rest, it is necessary to use various statistical techniques.

One fundamental, but rarely used, method for obtaining distances to Galactic PNe is through the photometric parallaxes of resolved companion stars. Perhaps two-thirds of all stars are members of binary systems, and the evidence suggests that the orbital period distribution of these binaries is a Gaussian in log P centered at $P \approx 180$ yr, with a disper-

[1] Department of Astronomy and Astrophysics, Pennsylvania State University, 525 Davey Laboratory, University Park, PA 16802; rbc@astro.psu.edu, sipior@astro.psu.edu.
[2] Space Telescope Science Institute, 3700 San Martin Drive, Baltimore, MD 21218; bond@stsci.edu.
[3] Current address: Observatoire de Genève, CH-1290 Sauverny, Switzerland; Laura.Fullton@obs.unige.ch.
[4] Current address: Department of Physics and Astronomy, University of Calgary, Calgary, Alberta, Canada T2N 1N4; zhangc@acs.ucalgary.ca.
[5] Current address: Department of Physics, Astronomy and Geosciences, Towson University, Towson, MD 21252; kschaef@towson.edu.
[6] Based on observations with the NASA/ESA *Hubble Space Telescope*, obtained at the Space Telescope Science Institute, which is operated by the Association of Universities for Reasearch in Astronomy, under NASA contract NAS 5-26555.

sion of 2.3 in the logarithm of the period (Duquennoy & Mayor 1991). Main-sequence binaries with periods less than $\sim$1000 days, but still wide enough for a red giant to form, will eventually evolve through a common-envelope phase and produce systems with dramatically shorter periods or even a coalesced binary (see Bond & Livio 1990; Yungelson, Tutukov, & Livio 1993). However, stars with larger initial periods will not interact, and their separations will actually increase with time, as a consequence of stellar mass loss. As a result, it is likely that nearly half of all planetary nebula nuclei (PNNs) have wide binary companions.

Despite this expectation, only a few PNNs are actually known to have resolved visual companions. The best known case is the nucleus of NGC 246, which has a 14th magnitude K-dwarf companion 3″.8 away (Minkowski 1960; Cudworth 1973). Fitting of this companion to the main sequence provides what is generally accepted as one of the most accurate PN distances (quoted as 430 pc by Cahn, Kaler, & Stanghellini 1992, and revised to 495^{+145}_{-100} pc on the basis of CCD photometry by Bond & Ciardullo 1999) and one that is almost always used as a primary calibrator of statistical distance methods. Other PNNs reported to have resolved companions include those of NGC 650-1, A24, A30, and A33 (Cudworth 1973), NGC 3132 (Kohoutek & Laustsen 1977), NGC 6853 (Cudworth 1973, 1977), A63 (Krzeminski 1976), K1-14 (Kaler 1981), and PuWe 1 (Purgathofer & Weinberger 1980), but at the time of this survey, only the companion to NGC 3132 had photometry accurate enough to provide a reliable spectroscopic parallax (Pottasch 1980, 1984).

Here we present the results of a *Hubble Space Telescope* (*HST*) snapshot survey of Galactic planetary nebulae, designed to detect and measure resolved binary PNN companions. In § 2, we describe the survey and the photometric procedures used to measure all the stars present on our CCD frames. In § 3, we use these data to create a list of PNNs that have visual companions deserving of follow-up observations. In § 4, we discuss the issue of interstellar reddening and compare measures of extinction based on two-color photometry with estimates derived from the emission lines of the nebulae. In § 5, we transform our *HST* stellar magnitudes to the standard Landolt (1983, 1992) system and present V and I magnitudes for 109 central stars. Because of the superior resolving power of the *HST*, these magnitudes are generally better than PNN measurements made from the ground, especially for objects with $V > 15.4$. In § 6, we discuss our candidate binaries individually and derive distances to those systems that are most likely to be physically associated. Finally, in § 7, we compare our distances with estimates based on statistical methods and discuss the implications our observations have for the Galactic PN distance scale.

2. TARGET SELECTION, OBSERVATIONS, AND REDUCTIONS

Our observations were carried out as a "snapshot survey" during Cycles 3 and 5 of the *HST* General Observer program. *HST* snapshots are short exposures taken during occasional gaps that remain in the observing program after as many primary scientific observations as possible have been scheduled. The targets that are observed during these opportunities are selected at random from a list of candidates provided by the observers.

The PNe in our target pool were chosen using criteria designed to maximize our chances of finding resolved companion stars. First among these criteria was that the objects in our survey had to be nearby. Our target selection was heavily influenced by the list of very nearby PNe given by Terzian (1993), and nearly all of our targets have statistical distances from Cahn, Kaler, & Stanghellini (1992; hereafter CKS) and/or Zhang (1995) that are less than $\sim$3 kpc. Almost as important was our Galactic latitude criterion: in order to reduce contamination from superposed field stars, most of our targets were chosen to have $|b| > 10°$. A third selection criterion was known or suspected binarity of the central star. We included in our target list the nine PNNs with reported visual companions (as listed above), along with A34, A66, and Th 2-A, whose visual companions were noted by H. E. B. during ground-based observations. In addition we included seven central stars that have composite or late-type spectra but are unresolved from the ground and show no evidence for being extremely close binaries. Finally, to increase the usefulness of our data set for comparison with other distance techniques, we included six PNe with Very Large Array expansion distances (Hajian, Terzian, & Bignell 1993, 1995; Hajian & Terzian 1996), 15 nebulae with distance estimates based on model atmosphere analyses of their central stars (Méndez, Kudritzki, & Herrero 1992), and seven PNNs known to be very close binaries (A46, A63, A65, HFG 1, K1-2, LoTr 5, and NGC 2346; cf. Bond 1994), from which distances can potentially be obtained from light-curve solutions. In all, 144 PNNs were included in our input target lists.

Our snapshot images were taken with the *HST* between 1993 and 1997. The Cycle 3 (1993) observations were obtained with the Planetary Camera of the original Wide Field and Planetary Camera (WF/PC). These data consisted of single exposures through the F785LP ("I") filter plus occasional exposures through the F555W ("V") filter, usually with the PN central star positioned near the center of the PC6 CCD.

The Cycle 5 (1995–1997) data were obtained using the F814W ("I") and F555W ("V") filters of the Wide Field Planetary Camera 2 (WFPC2), with the CCD gain set at 14 e^- DN$^-$. For these observations the PNNs were centered on the Planetary Camera chip and usually imaged twice in each filter, with the second exposure typically being $\sim$2 times longer than the first. The uneven exposure times optimized our ability to detect binaries. We generally tried to scale our shorter integrations so that the PNN's image fell just short of saturation (i.e., $\sim$50,000 e^- in the central pixel); this insured an accurate measurement of the PNN's magnitude and color and enabled us to search for companions with $\Delta m \lesssim 4.5$ to within $\rho \sim 0''.05$ of the central star. Conversely, we attempted to scale our longer exposures so that the central pixel of the PNN could receive as much charge as possible ($\sim$100,000 e^-) without bleeding significantly into its neighboring pixels. By doing this, we could search for companions almost $\sim$7 mag fainter than the central star with $\rho \gtrsim 0''.3$ separation.

Because of the limited time available per snapshot visit, we imposed a maximum integration time of 900 s per filter. The second, deeper exposures in each filter described above were omitted if they would be longer than 500 s in F814W or 200 s in F555W. Exposures longer than 600 s were split into two equal-length integrations to aid in cosmic-ray removal. Because of the uncertainties of the ground-based

PNN magnitudes used to calculate our exposure times, we had anticipated that not all of our targets would be optimally exposed. In fact, however, most of our program PNNs had useful exposures, and we were able to perform a careful search for visual binaries around almost every object. There was a guide star acquisition error for our observation of Lo 4, which resulted in our obtaining only a single F555W exposure under gyro control.

A summary of the WF/PC and WFPC2 observations appears in Tables 1 and 2. Of the 144 objects in the target list, 113 were actually observed: 26 with WF/PC, 84 with WFPC2, and 3 with both.

Photometric reduction of our CCD images was accomplished using a combination of IRAF and DAOPHOT/ALLSTAR (Stetson 1987). After the standard STScI pipeline debiasing and flat-fielding, we removed charged-particle events ("cosmic rays") from the data. For this task, the Cycles 3 and 5 frames were handled differently. Because the Cycle 3 data consisted only of single exposures through the F785LP and F555W filters, we could not simply "stack" these images and remove discrepant pixels. Instead, we employed a semiautomatic iterative technique, which took advantage of the fact that stars on the original WF/PC frames had aberrated point-spread functions (PSFs). First, we filtered our images using a 7×7 moving window and masked all points that deviated by more than $3\ \sigma$ from the median defined by their surroundings. We then compared these filtered images with their parent images and carefully examined the cores of all stars on the frames. If the filtering algorithm had affected the cores, the original pixel values were manually inserted back into the images. In this way, the bulk of the cosmic rays were removed without affecting the stellar photometry.

Reduction of the WFPC2 data proceeded in a more standard manner. All the data were first multiplied by a corrective image, in order to compensate for the geometrical distortions present in the flat-field images. We then used the DAOPHOT routine FIND to produce a list of candidate objects for each frame. These lists were culled of cosmic-ray events and other spurious detections by first rejecting all objects that fell within the vignetted areas of the frames and then comparing the object lists derived from the individual frames of a given target. Objects found on the shorter exposures, but not on the longer ones, were discarded as cosmic rays.

Photometry of the WFPC2 data was performed via a PSF fitting technique. Using all the frames of our survey, we identified ~ 20 bright, isolated stars in each of the four CCD camera fields, and from these data we defined the instrument's position-dependent PSF. Once the PSF was defined, we used it to derive preliminary instrumental magnitudes and create star-subtracted images. If any poor subtractions were found, the result of either the presence of an undetected close binary or a poorly determined nebular background, the process was repeated with a modified star list and/or a model for the nebular emission (cf. Ciardullo & Bond 1996). The raw instrumental magnitudes derived by ALLSTAR were then scaled to an 11 pixel radius aperture using an aperture correction derived from the bright stars and corrected for the effects of finite charge transfer effi-

TABLE 1

PLANETARY NEBULAE OBSERVED IN CYCLE 3

NAME	PN G DESIGNATION	DATE OF OBSERVATION	EXPOSURE TIMES (s)	
			F555W	F785LP
A24	217.1 + 14.7	1993 Sep 25	230	1200
A30	208.5 + 33.2	1993 Nov 03	35	160
A46	055.4 + 16.0	1993 Aug 22	...	350
A63	053.8 − 03.0	1993 Oct 21	50	230
A82	114.0 − 04.6	1993 Aug 16	60	300
EGB 5	211.9 + 22.6	1993 Nov 07	...	100
H3-75	193.6 − 09.5	1993 Aug 18	60	300
He 1-5	060.3 − 07.3	1993 Nov 16	...	40
He 2-36	279.6 − 03.1	1993 Oct 24	8	40
HFG 1	136.3 + 05.5	1993 Sep 24	...	70
IC 289	138.8 + 02.8	1993 Oct 10	...	800
IC 1747	130.2 + 01.3	1993 Aug 17	...	400
IC 2448	285.7 − 14.9	1993 Sep 11	...	160
IC 4637	345.4 + 00.1	1993 Sep 22	...	30
IC 4997	058.3 − 10.9	1993 Sep 22	...	180
K1-16	094.0 + 27.4	1993 Sep 26	...	350
K2-15	263.2 + 00.4	1993 Oct 24	2	10
LoTr 5	339.9 + 88.4	1993 Nov 25	0.2	1
M1-2	133.1 − 08.6	1993 Sep 24	14	70
M1-26	358.9 − 00.7	1993 Sep 20	...	40
NGC 1514	165.5 − 15.2	1993 Oct 22	0.35	1.8
NGC 3587	148.4 + 57.0	1993 Oct 24	...	800
NGC 6905	061.4 − 09.5	1993 Oct 29	...	600
NGC 7009	037.7 − 34.5	1993 Oct 20	...	40
NGC 7026	089.0 + 00.3	1993 Oct 24	...	160
NGC 7094	066.7 − 28.2	1993 Nov 16	...	100
NGC 7293	036.1 − 57.1	1993 Nov 02	...	70
PuWe 1	158.9 + 17.8	1993 Oct 24	80	400
Vy 2-2	045.4 − 02.7	1993 Sep 16	...	230

TABLE 2

PLANETARY NEBULAE OBSERVED IN CYCLE 5

NAME	PN G DESIGNATION	DATE OF OBSERVATION	EXPOSURE TIMES (s)			
			F555W−1	F555W−2	F814W−1	F814W−2
A7	215.5 − 30.8	1995 Aug 17	50	100	200	350
A16	153.7 + 22.8	1995 Sep 15	300	…	400	400
A21	205.1 + 14.2	1995 Sep 29	80	160	350	500
A28	158.8 + 37.1	1995 Sep 24	300	…	400	400
A31	219.1 + 31.2	1995 Nov 19	50	100	200	350
A33	238.0 + 34.8	1996 Feb 13	50	100	200	350
A34	248.7 + 29.5	1995 Nov 27	100	…	400	…
A39	047.0 + 42.4	1995 Jul 28	60	120	230	400
A43	036.0 + 17.6	1995 Jul 28	26	50	100	160
A61	077.6 + 14.7	1995 Jul 24	300	…	400	400
A65	017.3 − 21.9	1995 Aug 12	80	160	300	500
A66	019.8 − 23.7	1995 Aug 13	300	…	400	400
A72	059.7 − 18.7	1995 Aug 31	80	180	350	…
A74	072.7 − 17.1	1995 Aug 20	230	…	400	400
A78	081.2 − 14.9	1995 Oct 25	6	12	23	40
EGB 1	124.0 + 10.7	1995 Sep 27	100	…	400	…
He 2-131	315.1 − 13.0	1995 Jul 31	0.8	1.6	3.5	5
He 2-138	320.1 − 09.6	1996 Aug 11	0.8	1.6	3	5
IC 418	215.2 − 24.2	1995 Sep 24	0.4	0.8	1.6	2.6
IC 2149	166.1 + 10.4	1995 Nov 06	1	2	4	7
IC 2448	285.7 − 14.9	1995 Oct 10	16	30	60	100
IC 3568	123.6 + 34.5	1995 Aug 04	5	10	20	30
IC 4406	319.6 + 15.7	1995 Jul 30	300	…	400	400
IC 4593	025.3 + 40.8	1995 Aug 28	1	2	4	7
IC 4637	345.4 + 00.1	1995 Sep 24	3.5	7	14	23
IC 4997	058.3 − 10.9	1995 Sep 14	20	40	80	120
IC 5148-50	002.7 − 52.4	1995 Sep 02	50	100	200	350
IsWe 1	149.7 − 03.3	1995 Nov 08	140	…	500	…
Jn 1	104.2 − 29.6	1995 Jul 29	100	180	350	…
JnEr 1	164.8 + 31.1	1995 Sep 19	180	…	350	350
K1-2	253.5 + 10.7	1995 Sep 26	100	…	400	…
K1-14	045.6 + 24.3	1996 Jan 22	120	…	500	…
K1-22	283.6 + 25.3	1995 Aug 08	80	180	350	…
K1-27	286.8 − 29.5	1995 Dec 04	160	…	600	…
Lo 4	274.3 + 09.1	1995 Sep 30	140	…	…	…
Lo 8	310.3 + 24.7	1995 Sep 09	5	10	20	35
M2-9	010.8 + 18.0	1997 May 24	12	23	100	180
Mz 2	329.3 − 02.8	1996 Aug 19	200	200	400	400
NGC 40	120.0 + 09.8	1995 Nov 10	1.4	3	6	10
NGC 650-1	130.9 − 10.5	1995 Aug 05	80	160	300	500
NGC 1360	220.3 − 53.9	1995 Dec 16	1.2	2.3	4	8
NGC 1501	144.5 + 06.5	1995 Sep 07	20	40	80	140
NGC 1535	206.4 − 40.5	1995 Nov 25	2.6	5	10	16
NGC 2022	196.6 − 10.9	1995 Aug 11	80	140	300	500
NGC 2346	215.6 + 03.6	1995 Oct 27	1.2	2.6	5	8
NGC 2371-2	189.1 + 19.8	1995 Oct 24	26	50	100	200
NGC 2392	197.8 + 17.3	1995 Nov 20	0.5	1	2	3.5
NGC 2440	234.8 + 02.4	1995 Nov 18	350	…	400	400
NGC 2452	243.3 − 01.0	1995 Sep 04	400	…	400	400
NGC 2610	239.6 + 13.9	1995 Oct 10	70	140	260	400
NGC 2792	265.7 + 04.1	1995 Aug 11	260	…	400	400
NGC 2867	278.1 − 05.9	1995 Jul 30	70	140	300	500
NGC 3132	272.1 + 12.3	1995 Dec 04	0.35	0.7	1.4	2.3
NGC 3195	296.6 − 20.0	1995 Oct 05	80	180	350	…
NGC 3242	261.0 + 32.0	1996 Feb 15	2.6	5	10	18
NGC 3918	294.6 + 04.7	1995 Oct 18	60	120	260	400
NGC 4361	294.1 + 43.6	1996 Dec 02	6	12	26	40
NGC 5189	307.2 − 03.4	1995 Sep 02	30	60	120	200
NGC 5307	312.3 + 10.5	1995 Jul 28	23	50	100	160
NGC 5315	309.1 − 04.3	1995 Jul 25	20	40	80	120
NGC 5882	327.8 + 10.0	1995 Jul 26	8	16	30	50
NGC 5979	322.5 − 05.2	1997 Feb 07	40	80	180	300
NGC 6026	341.6 + 13.7	1995 Sep 27	7	14	26	40

TABLE 2—*Continued*

Name	PN G Designation	Date of Observation	Exposure Times (s)			
			F555W−1	F555W−2	F814W−1	F814W−2
NGC 6058.....	064.6 + 48.2	1995 Oct 22	12	23	40	80
NGC 6153.....	341.8 + 05.4	1997 Jun 01	80	180	350	350
NGC 6309.....	009.6 + 14.8	1995 Aug 26	140	...	600	...
NGC 6369.....	002.4 + 05.8	1995 Aug 09	80	160	300	500
NGC 6543.....	096.4 + 29.9	1995 Nov 22	1	2	4	6
NGC 6578.....	010.8 − 01.8	1995 Aug 16	70	140	300	500
NGC 6629.....	009.4 − 05.0	1995 Aug 16	5	10	20	35
NGC 6720.....	063.1 + 13.9	1995 Sep 17	60	120	260	400
NGC 6781.....	041.8 − 02.9	1995 Jul 24	180	...	350	350
NGC 6790.....	037.8 − 06.3	1996 Aug 30	12	23	50	80
NGC 6804.....	045.7 − 04.5	1995 Sep 18	18	35	70	120
NGC 6826.....	083.5 + 12.7	1995 Aug 21	0.6	1.2	2.3	4
NGC 6853.....	060.8 − 03.6	1995 Oct 31	12	26	50	80
NGC 6884.....	082.1 + 07.0	1995 Oct 13	80	180	350	...
NGC 6891.....	054.1 − 12.1	1995 Nov 20	3	6	12	20
NGC 6894.....	069.4 − 02.6	1995 Jul 28	500	...	400	400
NGC 7008.....	093.4 + 05.4	1995 Aug 24	6	12	26	40
NGC 7009.....	037.7 − 34.5	1997 May 28	4	120	18	180
NGC 7027.....	084.9 − 03.4	1995 Aug 21	100	200	400	...
NGC 7662.....	106.5 − 17.6	1995 Sep 27	6	12	26	40
PHL 932.....	125.9 − 47.0	1995 Jul 28	2.3	5	10	16
RX J2117+34.....	080.3 − 10.4	1995 Nov 21	6	12	26	40
Sp 3	342.5 − 14.3	1995 Sep 13	3.5	7	14	23
Th 2-A	306.4 − 00.6	1995 Sep 22	20	40	80	140

ciency following the prescription of Holtzman et al. (1995). Finally, the WFPC2 magnitudes were corrected for a nonlinear term related to integration time (Casertano 1997) and put on the photometric system defined by Holtzman et al.

Because the aberrated WF/PC images had a brighter limiting magnitude than their WFPC2 counterparts, there were, in general, fewer stars on these frames, and saturation in the stellar cores was less of a problem. Thus, our photometric techniques were simpler. In most cases, photometry was accomplished by summing the flux of each star within an aperture of radius 5 pixels; only when the stellar separations were of the order of a few pixels, or when the stellar cores were saturated, were DAOPHOT's PSF fitting routines used. The small-aperture measurements were then converted to total instrumental magnitudes using aperture corrections found from bright stars and scaled to the *HST* standard system using the ground-based WF/PC calibration of Harris et al. (1991) and the flight calibration of Hunter et al. (1992). Finally, depending on the Julian Date of the observation, an additional correction of up to 0.1 mag was applied to the F555W magnitudes, in order to account for the WF/PC chips' loss of sensitivity with time due to contamination (cf. Ritchie & MacKenty 1993, 1994).

3. DETECTION OF BINARIES

Because our data contain no information about proper motion or radial velocity, our assignment of physical binarity has to rely solely on the spatial coincidence of stars. The probability of our identifying a binary PNN depends critically both on the apparent separation of the companion star and on the field star surface density. (In other words, in a sufficiently crowded field even a closely separated physical pair would be mistaken for an optical double.) To improve our chances of detecting visual binaries, our target sample was weighted toward objects at high galactic latitude and toward nearby objects, as described above. Still, because the surface density of bright stars is much lower than for faint stars, our analysis is significantly more sensitive to brighter companions than to fainter ones.

To estimate whether a given apparent companion star located near a PNN is physically associated with it, we calculate the Poisson probability P that a random field star as bright as, or brighter than, the companion would be projected by chance within a radius ρ of the PNN. Mathematically,

$$P = 1 - \left(1 - \frac{\pi\rho^2}{A}\right)^N , \quad (1)$$

where A is the total sky area surveyed by each WF/PC or WFPC2 frame, and N is the number of stars within this area that are at least as bright as the companion. P is a function of the local stellar surface density, which we determined directly from star counts on the frames.

If true physical binaries are common in our sample, there should be an excess of pairs with very low values of P. (It was, of course, just such an argument, first made by Michell 1767, that established the existence of physical double stars.) In Figure 1, we plot the distribution of P for our sample of PNNs, using the stellar neighbor of each central star that has the lowest value of P (i.e., the highest probability of being physically associated; generally, but not always, this is also the nearest neighbor of the PNN). If all of our frames were populated entirely by randomly distributed field stars, without any true physical pairs, the distribution would be flat; instead, Figure 1 shows a large excess of companions with very small chance probabilities, particularly for $P \leq 0.05$. This is a clear demonstration that we are detecting true resolved physical doubles.

We therefore chose all of the apparent binaries with a chance probability of 5% or less for further investigation

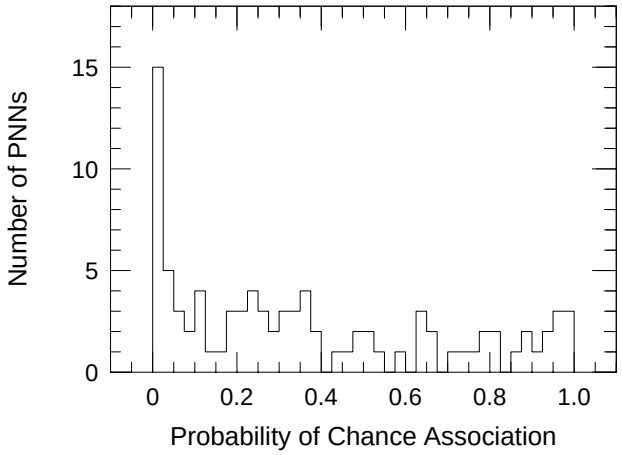

FIG. 1.—Histogram showing the distribution of probabilities for the hypothesis that the most likely companion to each of our PNNs is actually a randomly superposed field star. If physical binaries did not exist, the distribution would be flat. Instead, there is a large excess of PNNs with nearby companions ($P \leq 0.05$). These objects are listed in Table 3 and are discussed in this paper. The small excess in the range $0.05 < P < 0.40$ suggests that some additional physical pairs with larger separations still await discovery.

and list them in Table 3. Most of the columns are self-explanatory. Columns (2) and (3) give the separation, ρ, between the PNN and the candidate companion and the J2000.0 position angle of the companion with respect to the central star, respectively. Column (8) presents the probability P of a chance projection, as calculated from equation (1). To give an indication of the uncertainty in the probability, we give in the final column of Table 3 the value of P calculated by increasing the local stellar density by 1 σ above that deduced directly from the star counts.

Table 3 is *not* necessarily a list of true binary PNNs: it is merely the complete set of objects that, formally, have more than a 95% probability of being a physical pair. Since we imaged over a hundred PNNs in the course of this survey, we can expect ~ 6 chance superpositions to be contained in the list. In § 6, we will examine the properties of the PNNs in question and attempt to select those systems that are most likely to be true physical pairs.

Returning to Figure 1, we note that in addition to the sharp peak at small probabilities, there is a slight excess of objects with chance probabilities between 0.05 and 0.40. This suggests that a few additional PNNs not included in Table 3 also have physical companions. Unfortunately, because the ratio of true binaries to chance superpositions in this probability range is low, the only way to identify these objects would be through proper motion and/or radial velocity measurements of the candidate companions.

4. INTERSTELLAR EXTINCTION

The first step in deriving distances from two-color photometry is to obtain an estimate of the amount of interstellar extinction suffered by each object. This can be done in two ways.

The first method is to use the observed emission ratios (i.e., the relative intensities of Hα, Hβ, and the radio continuum) in the PNNs' surrounding nebulae. The intrinsic Hα-to-Hβ ratio of a typical 10,000 K nebula is ~ 2.86 (e.g., Brocklehurst 1971); by comparing this value with the observed line ratio, it is possible to compute the logarithmic extinction at Hβ, denoted c. Similarly, an estimate of c can be obtained by comparing the nebula's radio continuum (measured at 5 GHz) to its total emission at Hβ (cf. Milne & Aller 1975). Measures of c exist in the literature for a large number of objects, and a useful compilation appears in CKS. Unfortunately, because most PNe exhibit complex

TABLE 3

CANDIDATE COMPANION STARS

NAME	SEPARATION (arcsec)	J2000.0 P.A. (deg)	F814W	F555W − F814W	V	$V-I$	PROBABILITY Observed	PROBABILITY $+1\ \sigma$
A7	0.91	250	21.16	>1.20	>22.34	>1.21	0.005	0.006
A24	3.33	159	17.27[a]	1.34	18.55	1.16	0.021	0.033
A30	5.25	144	16.33[a]	1.11	17.40	0.97	0.035	0.058
A31	0.26	242	18.94	>3.12	>22.17	>3.17	0.001	0.001
A33	1.82	209	15.92	1.16	17.06	1.18	0.017	0.021
A63[a]	2.82	94	14.61	1.31	15.87	1.13	0.015	0.024
IC 4637	2.42	330	13.22	1.39	14.60	1.41	0.034	0.041
K1-14	0.36	242	17.61	1.03	18.63	1.04	0.001	0.001
K1-22	0.35	218	16.02	1.11	17.13	1.12	0.001	0.001
K1-27	0.56	315	20.93	0.36	21.29	0.37	0.009	0.010
Mz 2	0.28	218	15.85	1.23	17.06	1.25	0.000	0.000
NGC 650-1[b]	1.34	185	17.42	1.06	18.45	1.07	0.047	0.051
	1.45	190	18.22	1.06	19.25	1.07		
NGC 1535	1.04	334	16.75	0.93	17.65	0.94	0.002	0.002
NGC 2392	2.65	213	16.85	>0.51	>17.34	>0.52	0.012	0.017
NGC 2610	0.61	277	21.89	>0.78	>22.64	>0.79	0.008	0.009
NGC 3132	1.71	47	10.00	0.12	10.11	0.12	0.001	0.001
NGC 7008	0.42	241	13.10	1.32	14.40	1.34	0.001	0.001
PuWe 1[b]	5.20	119	13.20[a]	1.60	14.74	1.38	0.034	0.057
	5.45	113	15.89	3.43	19.22	2.92		
Sp 3	0.31	42	16.06	0.82	16.86	0.83	0.002	0.002

[a] Magnitude through the WF/PC F785LP filter.
[b] The companion to the PNN is itself a binary.

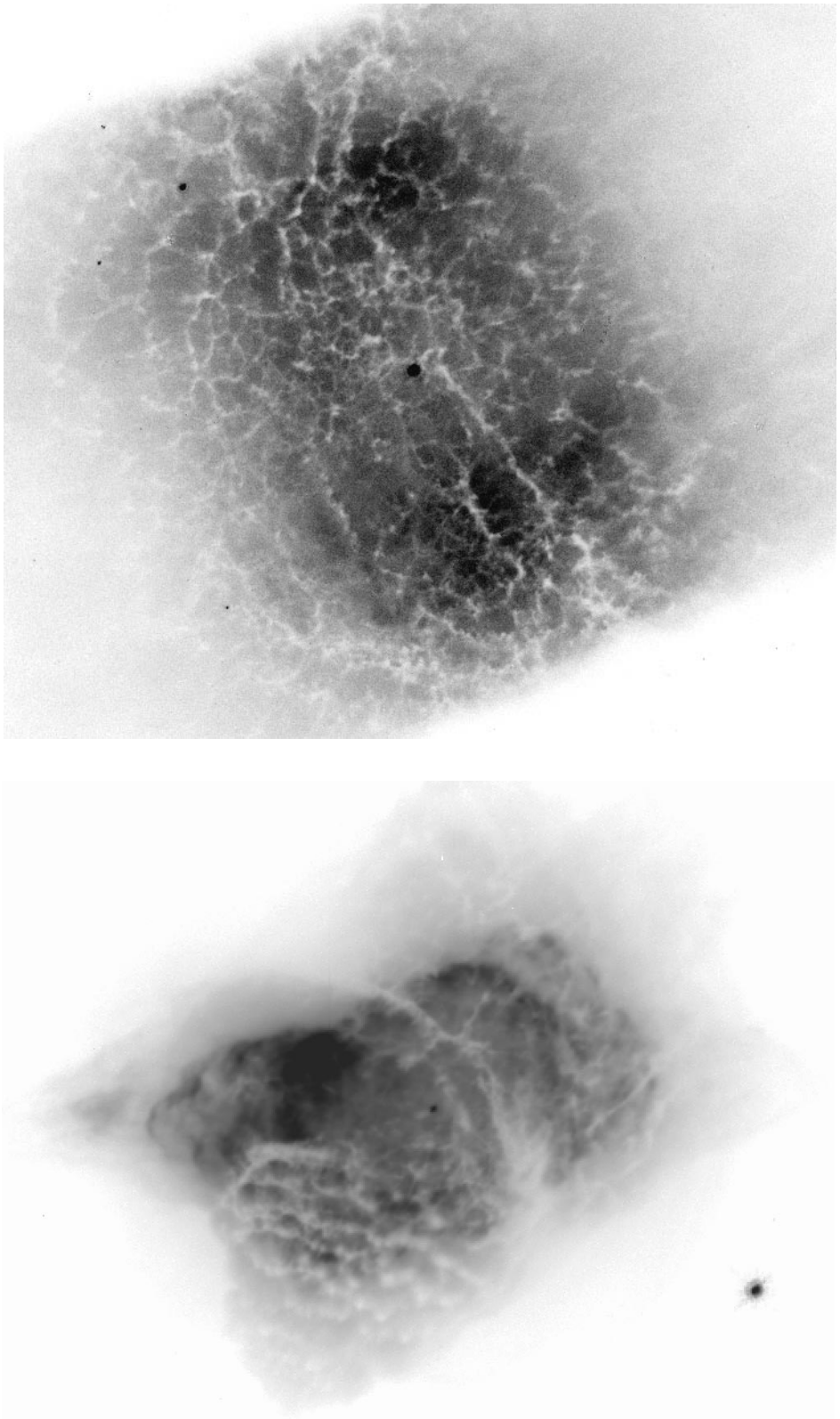

FIG. 2.—*HST* WFPC2 *V*-band images of NGC 7027 (*bottom*) and IC 4406 (*top*). For NGC 7027 a logarithmic stretch has been used to display the image because of the large range of surface brightness. Angular widths of the images are 23″ (*bottom*) and 33″ (*top*). Note, at *HST* resolution, the presence of extremely patchy and filamentary dust features in both planetary nebulae. Because of this small-scale structure, an extinction measurement based upon global nebular properties, or even upon the colors of a central star, might not be appropriate for a nearby resolved companion.

multizone structures, the exact values to use for the intrinsic Hα/Hβ and Hβ/radio ratios can be difficult to determine; in addition, observational errors introduced by atmospheric dispersion, background confusion (for radio-faint PNe), and uncertain emission-line photometry (for large, low surface brightness PNe) can lead one astray. Finally, as our *HST* images of NGC 7027 and IC 4406 in Figure 2 show, the dust within a PN can be extremely patchy. Thus, adoption of a

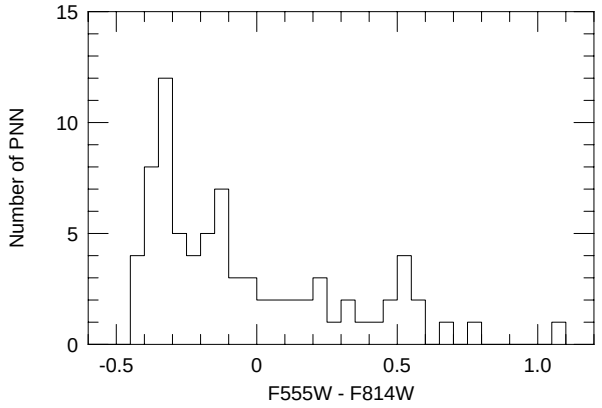

FIG. 3.—Distribution of colors for PNNs observed with WFPC2, excluding those objects with composite or late-type spectra. The blue limit of the distribution, F555W − F814W $\simeq -0.4$, agrees with the color predicted for an infinitely hot, unreddened blackbody.

global extinction value for the particular line of sight to the central star (or to its companion) may not be appropriate.

The second method of determining the extinction to a PNN is to compare the observed color of the central star with that expected from a hot source. Simulations using the WFPC2 efficiency curves (Biretta et al. 1996) demonstrate that a star whose optical continuum falls on the Rayleigh-Jeans tail of the Planck function should have an F555W − F814W color of roughly −0.4. As the histogram of Figure 3 illustrates, this value is confirmed in our survey: the distribution of PNN colors observed with WFPC2 has a hard blue limit of F555W − F814W ~ -0.4 and a long tail to the red caused by interstellar (and/or circumstellar) reddening. Values for the extinction of each PNN can therefore be obtained directly from our measured colors. Of course, some of the same uncertainties that affect the nebula-based extinction ratios apply here: spectroscopy demonstrates that there are real departures from Rayleigh-Jeans continua in some objects (e.g., from Wolf-Rayet emission lines; see, for example, Smith & Aller 1969; Heap 1982; Méndez et al. 1986). Moreover, some PNNs have intrinsically red colors (either from an unresolved late-type companion or because they themselves have evolved back to a "born-again" red giant phase). Finally, even if all central stars were identical, small-scale nonuniformities in the dust distribution (such as seen in Fig. 2) could cause a companion star to have a different reddening value than the hot component.

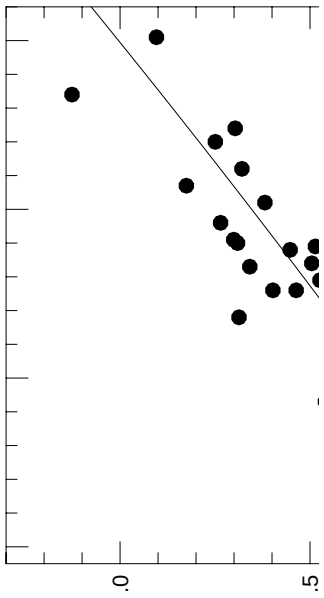

FIG. 4.—Comparison of extinction estimates based on PNN colors with those derived from the nebulae. The solid line is the relation derived by reddening a 100,000 K Planck curve and folding it through the F555W and F814W filter response curves. Both the PNN color extinctions and the theoretical relation have been transformed from E(F555W − F814W) to $E(B-V)$ using the table of Holtzman etal. (1995). PNNs with composite or late-type spectra have not been plotted. Note that although the relation between c and $E(B-V)$ is good in the mean there is a substantial dispersion in the measurements, with $\sigma_{E(B-V)} = 0.16$ mag.

Figure 4 compares the nebular extinction measurements (taken from CKS and Kingsburgh & Barlow 1994) with reddenings derived from our WFPC2 photometry using the assumption that the intrinsic F555W − F814W color of the central star is −0.40. For the figure, E(F555W − F814W) has been transformed to $E(B-V)$ using the extinction table for an O6 star given by Holtzman et al. (1995). In the figure, M2-9 and NGC 2022 have not been plotted, since both of their nuclei are marginally nonstellar on our *HST* frames and are probably surrounded by thick circumstellar dust. In addition, PNNs with known composite or late-type spectra have been omitted from the diagram. In those cases where the PN has both a radio flux value and Balmer decrement value for c, we have used the mean of the two measurements (except for Mz 2, whose Balmer decrement extinction of zero is clearly unphysical given the object's other properties).

The line in Figure 4 plots the relation between $E(B-V)$ and c derived by reddening a 100,000 K Planck curve with the Cardelli, Clayton, & Mathis (1989) extinction law, folding the resultant energy distribution through the F555W and F814W system response curves, and transforming from E(F555W − F814W) to $E(B-V)$ using the table of Holtzman et al. (1995). This relation has a slight curvature due to shifts in effective filter wavelength with increasing extinction (e.g., Kaler & Lutz 1985). An excellent approximation to this curve is

$$E(\text{F555W} - \text{F814W}) = 0.913c - 0.012c^2 \, . \qquad (2)$$

As can be seen in Figure 4, this law fits the data reasonably well in the mean, as the average difference between the two reddening estimators is $\Delta E(B-V) = 0.00 \pm 0.02$. However, it is also obvious that there is a substantial amount of scatter; the dispersion about the relation is $\sigma_{E(B-V)} = 0.16$ mag. Interestingly, this scatter is not confined to highly reddened PNe: even for those objects with $c < 0.2$ the scatter is still substantial, $\sigma_{E(B-V)} = 0.13$.

Without additional information, it is impossible to determine whether the scatter in Figure 4 is due principally to errors in the nebular extinction values or uncertainties associated with our PNN colors. In some individual cases, we can test whether the nebular extinction is reasonable by computing the dereddened color of the central star: if the application of c results in a color that is significantly bluer than the Rayleigh-Jeans limit, then the extinction has obviously been overestimated. However, from the data at hand, there is no reason to believe that one extinction estimate is better than the other. For simplicity, we therefore assume that both methods have similar uncertainties, of order $\sigma_{E(V-I)} \simeq 0.11$ mag. If a planetary nebula has both a color-

estimated reddening and a reasonable value for the nebular reddening, then we use the mean of these two numbers and assign an uncertainty of $\sigma_{E(V-I)} = 0.11/2^{1/2} = 0.08$ mag. If no measurements of the nebula exist, if the value of c leads to an implausible color for the central star, or if the PNN is known to have a composite or late-type spectrum (or poor photometry), then we use a reddening based solely on the remaining valid method and assume that $\sigma_{E(V-I)} = 0.11$ mag.

5. TRANSFORMATION TO V AND I

The final step before deriving PNN distances from binaries is to transform the photometric systems defined by the WF/PC and WFPC2 filters to the Johnson-Kron-Cousins V and I system as defined by the standard stars of Landolt (1983, 1992). For the WFPC2 data, this was done using the equations given by Holtzman et al. (1995), which should be good to $\sim$2% for colors in the range $-0.3 < V-I < 1.5$. Note that the bluest of our PNNs actually lie slightly outside this range at $V-I \approx -0.4$, and the transformations for these stars are not formally applicable. However, as the Holtzman et al. data for the extremely blue stars of ω Cen and the blue spectrophotometric standards Grw $+70°5824$, Feige 110, and AGK $+81°266$ show, the equations relating F555W and F814W to V and I are well behaved at the blue end and produce residuals that are no worse than those for stars of moderate color. Hence our mild extrapolation for the central stars should be valid.

Transformation equations are also available for the original WF/PC filter set (cf. Harris et al. 1991; Saha et al. 1994). However, these relations are only defined for stars with $B-V$ colors between 0.0 and 1.6. Since many of our nuclei are much bluer than this, we chose not to use these equations directly. Instead, we rederived the transformations for V and I by combining the red star data of Harris et al. (1991) with observations of his six blue Landolt standards: G162-66, GD 108, G163-50, G93-48, Feige 67, and SA 114-750. The resulting transformation equations, which are valid in the range $-0.5 <$ F555W $-$ F785LP < 3, are

$$\text{F785LP}-I = 0.054-0.154\,(V-I)-0.002\,(V-I)^2\,, \quad (3)$$

$$\text{F555W}-V = 0.001+0.061\,(V-I)-0.009\,(V-I)^2\,. \quad (4)$$

Both equations have rms residuals of 0.023 mag.

We note here that ground-based photometry of central stars within high surface brightness nebulae can be extremely difficult because of the bright, irregularly distributed flux from their surrounding nebulae (see Ciardullo & Bond 1996 for a discussion of this well-known problem). However, the superior resolving power of the *HST* reduces this problem enormously. Consequently, the V and I magnitudes obtained in our survey represent a useful new database for future PN analyses, even for the majority of stars that are not resolved binaries.

Our measured PNN V magnitudes and $V-I$ colors are listed in Table 4; for reference, the nebula-based values of c (which are taken from literature measurements of the Balmer decrement and/or radio flux density) are also tabulated. Table 5 lists the PNN I magnitudes for those objects not observed in V; except for the composite and late-type stars A46, He 1-5, and HFG 1, these data were transformed to the standard system using the nebula-derived value of c and the assumption that the intrinsic $V-I$ color of the objects is -0.4. (Abell 46, He 1-5, HFG 1 were transformed

TABLE 4

V MAGNITUDES, COLORS, AND EXTINCTIONS OF PNNs

Name	PN G Designation	V	$V-I$	c
A7	215.5 − 30.8	15.58	−0.34	...
A16	153.7 + 22.8	18.70	−0.14	0.47
A21	205.1 + 14.2	16.05	−0.33	0.18
A24	217.1 + 14.7	17.48	−0.38	0.48
A28	158.8 + 37.1	16.43	−0.44	0.00
A30	208.5 + 33.2	14.38	−0.15	0.00
A31	219.1 + 31.2	15.53	−0.42	0.00
A33	238.0 + 34.8	16.03	−0.44	0.13
A34	248.7 + 29.5	16.47	−0.35	0.20
A39	047.0 + 42.4	15.72	−0.24	0.00
A43	036.0 + 17.6	14.77	−0.09	0.59
A61	077.6 + 14.7	17.47	−0.22	...
A63	053.8 − 03.0	15.14	+0.36	0.71
A65	017.3 − 21.9	15.80	+0.41	0.00
A66	019.8 − 23.7	18.17	−0.12	...
A72	059.7 − 18.7	16.10	−0.33	0.54
A74	072.7 − 17.1	17.44	−0.03	...
A78	081.2 − 14.9	13.26	−0.19	0.18
EGB 1	124.0 + 10.7	16.39	−0.13	...
H3-75	193.6 − 09.5	14.24	+1.16	...
He 2-36	279.6 − 03.1	11.48	+0.83	1.18
He 2-131	315.1 − 13.0	10.97	+0.08	0.20
He 2-138	320.1 − 09.6	11.03	+0.06	0.28
IC 418	215.2 − 24.2	10.23	+0.01	0.32
IC 2149	166.1 + 10.4	11.34	+0.02	0.40
IC 2448	285.7 − 14.9	14.26	−0.28	0.11
IC 3568	123.6 + 34.5	12.97	−0.10	0.19
IC 4406	319.6 + 15.7	17.38	−0.14	0.28
IC 4593	025.3 + 40.8	11.33	−0.19	0.07
IC 4637	345.4 + 00.1	12.70	+0.55	1.00
IC 5148-50	002.7 − 52.4	16.16	−0.43	0.38
IsWe 1	149.7 − 03.3	16.53	−0.13	...
Jn 1	104.2 − 29.6	16.17	−0.29	0.08
JnEr 1	164.8 + 31.1	17.16	−0.40	0.00
K1-2	253.5 + 10.7	16.83	+0.20	...
K1-14	045.6 + 24.3	16.21	−0.27	0.00
K1-22	283.6 + 25.3	16.83	−0.31	0.12
K1-27	286.8 − 29.5	16.13	−0.33	0.28
K2-15	263.2 + 00.4	12.04	+1.28	...
Lo 4	274.3 + 09.1	16.58	...	...
Lo 8	310.3 + 24.7	13.00	−0.33	...
LoTr 5	339.9 + 88.4	8.95	+1.00	0.00
M1-2	133.1 − 08.6	13.05	+1.10	1.11
M2-9	010.8 + 18.0	14.45	+1.29	1.10
Mz 2	329.3 − 02.8	18.32	+0.40	1.03
NGC 40	120.0 + 09.8	11.55	+0.27	0.80
NGC 650-1	130.9 − 10.5	17.57	−0.16	0.19
NGC 1360	220.3 − 53.9	11.34	−0.41	0.00
NGC 1501	144.5 + 06.5	14.36	+0.56:	1.11
NGC 1514	165.5 − 15.2	9.52	+0.81	0.92
NGC 1535	206.4 − 40.5	12.11	−0.35	0.11
NGC 2022	196.6 − 10.9	15.75	−0.39	0.46
NGC 2346	215.6 + 03.6	11.27	+0.26	0.75
NGC 2371-2	189.1 + 19.8	14.85	−0.31:	0.21
NGC 2392	197.8 + 17.3	10.63	−0.14	0.19
NGC 2440	234.8 + 02.4	17.49	−0.07	0.44
NGC 2452	243.3 − 01.0	17.46	+0.51	0.68
NGC 2610	239.6 + 13.9	15.97	−0.35	0.10
NGC 2792	265.7 + 04.1	16.89	+0.22	0.75
NGC 2867	278.1 − 05.9	16.03	+0.20	0.47
NGC 3132	272.1 + 12.3	15.76	−0.24	0.23
NGC 3195	296.6 − 20.0	17.78	−0.26	0.28
NGC 3242	261.0 + 32.0	12.32	−0.34	0.12
NGC 3918	294.6 + 04.7	15.49	+0.01	0.33
NGC 4361	294.1 + 43.6	13.26	−0.33	0.08

TABLE 4—*Continued*

Name	PN G Designation	V	$V-I$	c
NGC 5189.....	307.2 − 03.4	14.53	+0.18:	0.61
NGC 5307.....	312.3 + 10.5	14.74	+0.03	0.51
NGC 5882.....	327.8 + 10.0	13.42	+0.07	0.40
NGC 5979.....	322.5 − 05.2	16.37	+0.04	0.40
NGC 6026.....	341.6 + 13.7	13.33	+0.13	0.66
NGC 6058.....	064.6 + 48.2	13.85	−0.36	0.04
NGC 6153.....	341.8 + 05.4	15.55	+0.42	1.04
NGC 6309.....	009.6 + 14.8	16.31	...	0.85
NGC 6369.....	002.4 + 05.8	15.13	...	1.94
NGC 6543.....	096.4 + 29.9	11.29	−0.18	0.12
NGC 6578.....	010.8 − 01.8	15.68	+0.78:	1.40
NGC 6629.....	009.4 − 05.0	12.87	+0.51:	0.90
NGC 6720.....	063.1 + 13.9	15.78	−0.38	0.20
NGC 6781.....	041.8 − 02.9	16.86	+0.41	1.12
NGC 6790.....	037.8 − 06.3	16.13	+0.53	0.81
NGC 6804.....	045.7 − 04.5	14.17:	+0.53:	0.87
NGC 6826.....	083.5 + 12.7	10.68	−0.24	0.04
NGC 6853.....	060.8 − 03.6	14.09	−0.46	0.11
NGC 6884.....	082.1 + 07.0	16.71	+0.49	0.81
NGC 6891.....	054.1 − 12.1	12.34	−0.16	0.23
NGC 6894.....	069.4 − 02.6	18.32	+0.33	0.79
NGC 7008.....	093.4 + 05.4	13.89	+0.21	0.66
NGC 7009.....	037.7 − 34.5	12.87	−0.23	0.14
NGC 7027.....	084.9 − 03.4	16.53	+0.47:	1.31
NGC 7662.....	106.5 − 17.6	14.00	−0.23	0.17
PHL 932.....	125.9 − 47.0	12.12	−0.31	...
PuWe 1	158.9 + 17.8	15.64	−0.27	0.23
RX J2117+34.....	080.3 − 10.4	13.10	−0.40	...
Sp 3	342.5 − 14.3	13.20	−0.19	...
Th 2-A	306.4 − 00.6	17.08	+0.71	1.07

using ground-based colors.) In most cases, the magnitudes listed in the tables are accurate to better than ∼0.05 mag and represent mean values derived from our two exposures. In a few cases, partially saturated stellar images compromised our ability to derive an accurate magnitude for the PNN. For the objects where this occurred, we double-checked our measurements by deriving both a PSF magnitude and an aperture-photometry magnitude and intercomparing the results computed from our long-exposure frame with those obtained from the short exposure. Those PNNs with uncertain magnitudes and colors are noted in Tables 4 and 5 with colons.

TABLE 5

I MAGNITUDES AND EXTINCTIONS OF PNNs

Name	PN G Designation	I	c
A46.....	055.4 + 16.0	15.48	0.00
EGB 5	211.9 + 22.6	14.36	...
He 1-5	060.3 − 07.3	10.22	0.60
HFG 1.....	136.3 + 05.5	13.00	0.55
IC 289	138.8 + 02.8	15.92	1.24
IC 1747	130.2 + 01.3	15.45	0.93
IC 4997	058.3 − 10.9	11.91	0.45
K1-16	094.0 + 27.4	15.48	0.57
M1-26.....	358.9 − 00.7	11.32	1.48
NGC 3587.....	148.4 + 57.0	17.15	0.07
NGC 6905.....	061.4 − 09.5	14.74	0.19
NGC 7026.....	089.0 + 00.3	13.62	0.76
NGC 7094.....	066.7 − 28.2	13.92	0.31
NGC 7293.....	036.1 − 57.1	14.03	0.00
Vy 2-2	045.4 − 02.7	12.12	1.39

Two central stars, those of IC 4997 and NGC 5315, were so badly overexposed that we were unable to derive V and I magnitudes; and two more, NGC 6309 and NGC 6369, were too badly overexposed in the I band only. For A82 we are uncertain of the identity of the central star, as discussed in detail below.

Figure 5 compares our *HST* V magnitudes with ground-based measurements obtained by Kaler and collaborators (Shaw & Kaler 1985, 1989; Jacoby & Kaler 1989) and by

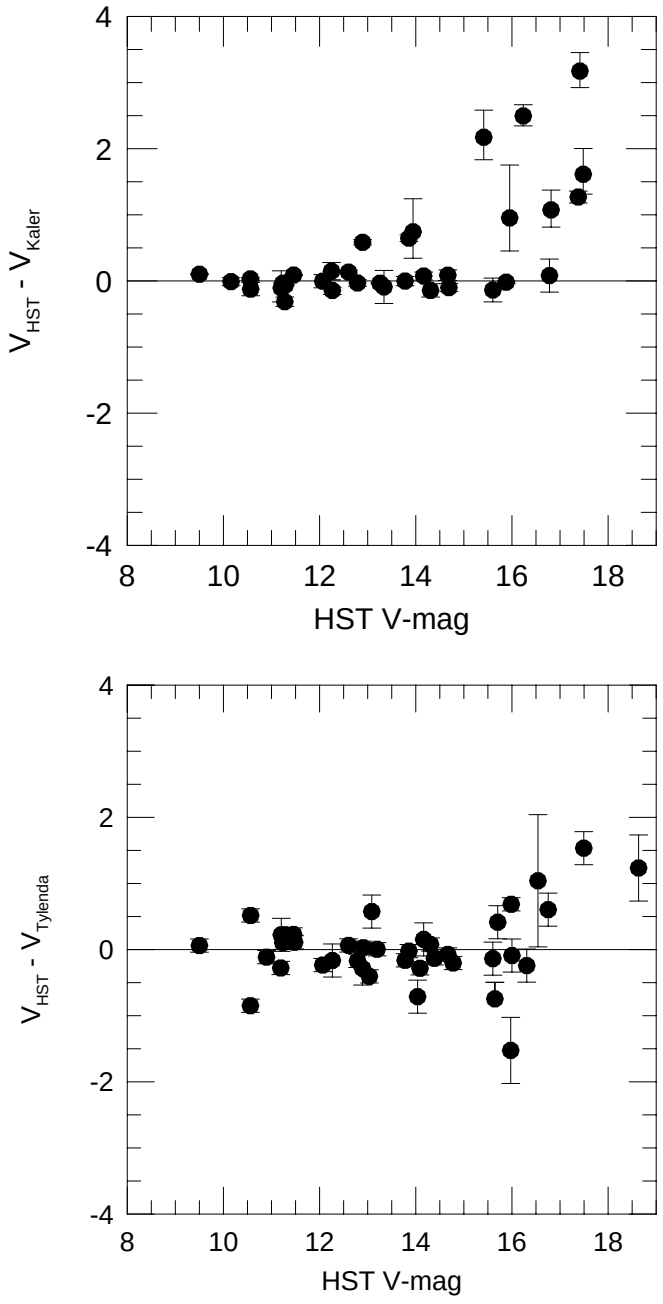

FIG. 5.—PNN V magnitudes derived from our *HST* measurements compared with the ground-based V magnitudes of Kaler and collaborators (Shaw & Kaler 1985, 1989; Jacoby & Kaler 1989) and Tylenda et al. (1991). For objects brighter than $V \simeq 15.4$, the agreement is good, although the scatter is slightly larger than would be predicted from the individual error bars. At fainter magnitudes large excursions exist, showing that some ground-based photometry has been severely contaminated by nebular emission.

Tylenda et al. (1991). The figure demonstrates that for PNNs with magnitudes brighter than $V \sim 15.4$, the agreement is generally good. There is no systematic error between our measurements and those of Tylenda et al., as the mean difference between the two magnitude systems is 0.00 ± 0.06 mag. Moreover, although our *HST* magnitudes are systematically fainter than the Kaler et al. measurements, the offset is small: when the highly discrepant objects IC 3568, NGC 7662, and NGC 7008 (which we resolve as a binary with two comparably bright components) are omitted, the mean difference between the two systems is 0.05 ± 0.03 mag. We note that, in general, the scatter between our measurements and those of Kaler et al. is significantly smaller ($\sigma \simeq 0.13$ mag) than that for Tylenda et al. ($\sigma \simeq 0.32$ mag). But, more importantly, both sets of residuals are larger than the internal errors of the measurements would indicate. Some of this additional scatter undoubtedly comes from intrinsic variability in the PNNs themselves, as Bond & Ciardullo (1990) and others have shown that ~ 0.1 mag variability in PN central stars is not uncommon.

For PNNs fainter than $V \simeq 15.4$, the agreement between the *HST* data and the ground-based measurements is considerably poorer. This is presumably due to the increased importance of nebular contamination in the ground-based photometry. The effect is particularly noticeable in the Kaler et al. data, where V-band fluxes derived from aperture photometry are overestimated by as much as ~ 3 mag.

6. PHYSICAL ASSOCIATIONS AND OPTICAL DOUBLES

The goal of this paper is to determine distances to PNe with resolved binary nuclei by fitting the companion stars to the main sequence. To do this, one should, in principle, use a main sequence appropriate for the metallicity of each individual nebula. However, of the candidates listed in Table 3, fewer than half have nebular abundance measurements, and of those, only ~ 5 have reliable data on atomic species that can reasonably be assumed to have been unaffected by nuclear processing. We have therefore chosen not to attempt any metallicity correction. Moreover, since most PNe arise from an old-disk population, we have also chosen not to use a main sequence based on observations of young, metal-rich clusters such as the Hyades or Pleiades. Instead, for our distance estimates, we use an M_V, $V-I$ main sequence that is derived from a spline fit to a color-magnitude diagram of old-disk field stars. This relation, which has kindly been provided to us by H. C. Harris (1998, private communication), is based on US Naval Observatory (USNO) CCD parallaxes of faint field stars (Monet et al. 1992; Dahn 1993; plus recent unpublished measurements), USNO photographic parallaxes of bright stars (Dahn et al. 1988), and a combination of data on large-parallax stars from other observatories. Since the data set excludes known halo objects, high-velocity stars, and binaries, the resultant main sequence should be applicable directly to our PN companions. The adopted USNO main sequence is given in Table 6.

As mentioned above, our candidate binary PNNs were selected purely on the basis of spatial coincidence. Hence, it is likely that a few optical doubles are mixed in with the true physical pairs. Although it is impossible to state with complete certainty whether any individual object is a binary, we can make some plausibility arguments based on the inferred properties of the stars and nebulae.

TABLE 6

ADOPTED MAIN SEQUENCE[a]

$V-I$	M_V	$V-I$	M_V
−0.10.....	0.0	2.40.....	10.53
0.00	0.77	2.50.....	10.85
0.10	1.50	2.60.....	11.16
0.20	2.15	2.70.....	11.55
0.30	2.75	2.80.....	12.10
0.40	3.32	2.90.....	12.70
0.50	3.85	3.00.....	13.22
0.60	4.36	3.10.....	13.65
0.70	4.85	3.20.....	14.02
0.80	5.35	3.30.....	14.35
0.90	5.80	3.40.....	14.64
1.00	6.18	3.50.....	14.91
1.10	6.50	3.60.....	15.19
1.20	6.81	3.70.....	15.47
1.30	7.12	3.80.....	15.75
1.40	7.42	3.90.....	16.03
1.50	7.73	4.00.....	16.30
1.60	8.04	4.10.....	16.58
1.70	8.35	4.20.....	16.87
1.80	8.66	4.30.....	17.14
1.90	8.97	4.40.....	17.39
2.00	9.28	4.50.....	17.70
2.10	9.58	4.60.....	18.14
2.20	9.88	4.70.....	18.65
2.30	10.20		

[a] From H. C. Harris 1998, private communication.

Table 7 lists inferred properties of all of our candidate binaries, grouped according to our belief that the physical association is probable, possible, or doubtful. The reasons for our categorization are given case-by-case below. To derive the distance moduli given in column (3), we dereddened the stars using the adopted $E(B-V)$ of column (2) and the prescriptions given by Harris et al. (1991) and Holtzman et al. (1995). We then fitted the dereddened companion(s) to the USNO main sequence of Table 6. Column (4) lists the formal errors in the derived distance moduli; these were calculated by combining in quadrature our photometric errors, the errors associated with the PNN reddening estimates, and the uncertainty in the main-sequence M_V value. Note that this last term, which we assume to be ~ 0.3 mag, usually dominates the error. Due to the spread of field star metallicities and the effects of stellar evolution, the observed main sequence in the solar neighborhood has at least a spread of 0.3 mag (Perryman et al. 1995; Jaschek & Gómez 1998). Consequently, although the mean main sequence at any color may be well defined, individual distance determinations that are based only on two-color photometry must have at least this amount of error. In the future it should be possible to refine our distance estimates via metallicities deduced from spectroscopy and/or Strömgren photometry of the companion stars, but for the present, our individual PN distance measurements carry this substantial uncertainty.

Columns (6)–(9) in Table 7 give various properties of the stars and nebulae under the assumption the companion stars are, indeed, physically associated with their PNNs. Column (6) is the projected PNN companion star separation in astronomical units, column (7) is the physical size of the PNN's nebula as derived from the angular diameters

TABLE 7

BINARY PN DISTANCES AND OTHER PROPERTIES

Name	$E(B-V)$	$(m-M)_0$	$\sigma(m-M)$	Distance (kpc)	Separation (AU)	Nebula Diameter (pc)	PNN M_V	PN M_{5007}
Probable associations:								
A31	0.000	<8.24	...	<0.44	<115	<2.09	>7.29	...
A33	0.000	10.32	0.31	1.16	2110	1.52	5.71	2.82
K1-14	0.050	12.39	0.33	3.00	1080	0.68	3.66	3.47
K1-22	0.076	10.63	0.33	1.33	470	1.16	5.96	3.10
K1-27	0.052	8.35	0.53	0.47	260	0.10	7.61	8.66
Mz 2	0.654	11.67	0.48	2.16	600	0.24	4.54	−1.79
NGC 1535	0.061	11.81	0.37	2.31	2400	0.23	0.10	−2.46
NGC 3132	0.143	9.42	0.71	0.77	1310	0.11	5.87	−0.06
NGC 7008	0.457	7.84	0.43	0.37	160	0.15	4.56	1.82
Sp 3	0.159	11.88	0.53	2.38	740	0.41	0.80	1.98
Possible associations:								
A7	0.049	<15.52	...	<12.70	<11520	<46.8	> −0.10	...
A30	0.092	11.52	0.38	2.02	10580	1.24	2.57	1.20
A63	0.488	10.43	0.56	1.22	3440	0.24	3.20	5.17
IC 4637	0.701	8.50	0.45	0.50	1210	0.05	1.94	0.92
NGC 2392	0.162	<14.03	...	<6.41	<16970	<0.61	> −3.93	> −5.23
NGC 2610	0.053	<17.54	...	<32.18	<19630	<5.93	> −1.74	> −4.30
Doubtful associations:								
A24	0.014	11.88	0.31	2.38	7920	4.1	5.55	2.65
NGC 650-1.....	0.155	13.07	0.38	4.12	5520	1.34	3.99	−3.34
					5970			
PuWe 1.....	0.130	7.47	0.31	0.31	1620	1.82	7.77	...
	0.130	6.89	0.43	0.24	1300	1.39	8.35	...

listed in Acker et al. (1992), column (8) is the absolute V magnitude of the PNN, and column (9) is the nebula's absolute [O III] λ5007 magnitude, based on the line fluxes given by Acker et al. (1992). Following Jacoby (1989), we define

$$M_{5007} = -2.5 \log F_{5007} - 13.74 , \quad (5)$$

where the monochromatic flux, F_{5007}, is given in ergs cm^{-2} s^{-1}.

A discussion of the individual objects appears below.

6.1. *Probable Physical Pairs*

Abell 31.—The central star of Abell 31 lies within an extremely large (diameter 970″) nebula and has a very faint, close companion that is detected only on our I frames. The extremely red color of the companion, $(V-I)_0 \gtrsim 3.2$, places an interesting limit on the distance: in order to be on the main sequence, the companion star must be closer than ~440 pc. This compares with statistical distance estimates that range from 230 pc (CKS) to 1 kpc (Zhang 1995). The small projected separation derived for the pair (<115 AU) and the very low probability for chance superposition (0.07%) argue strongly for additional observations.

Abell 33.—The companion to Abell 33 was first detected by Cudworth (1973); the separation and position angle of the pair has not changed significantly since then. The low probability of a chance superposition and the reasonable implied parameters of the system suggest that the stars are physically associated. Additional evidence for this conclusion comes from the approximate agreement between our distance of 1.2 kpc and the statistical distance estimates of ~0.7 kpc (CKS), 1.6 kpc (Maciel 1984), and 2.9 kpc (Zhang 1995).

We note here that Abell 33 (and Abell 24) have the largest reddening discrepancies in our sample. According to the observed $V-I$ color of the central star, the extinction toward Abell 33 should be close to zero. However, Kaler, Shaw, & Kwitter (1990) have used the nebular emission lines to infer a total Hβ extinction of almost a magnitude. Because of the object's high galactic latitude, the low extinction values derived by earlier emission-line studies (Chopinet & Lortet-Zuckermann 1976; Kaler 1983), and the negative reddening implied by the ratio of radio to Hβ flux (CKS), we have chosen to ignore the Balmer-line extinction measurement for this object and have used $E(V-I) = 0$ in our calculations.

K1-14.—Prints of the Palomar Sky Survey (POSS) reveal that a pair of stars separated by 9.″1 is at the center of this nebula. H. E. B. noted this fact ~20 yr ago, as did Kaler (1981), and on this basis we included the object in our program. However, Kaler & Feibelman (1985) concluded that neither of these stars is the PNN: using both *International Ultraviolet Explorer* (*IUE*) observations and a large-scale ground-based plate provided to them by F. Sabbadin, these authors concluded that the actual central star of K1-14 is a fainter third object, lying *between* the two POSS stars. Our *HST* images confirm that the Kaler-Feibelman conclusion is correct: an extremely blue object lies ~2.″4 southwest of the brighter POSS star. (The PNN is invisible on the POSS prints because of the overlapping images of the field stars.) Remarkably, the hot star itself has a very close, even fainter companion 0.″36 away. The very small separation of *this* pair, coupled with the low stellar density in the field, argue strongly for a physical association. Our distance, obtained with main-sequence fitting, of ~3 kpc is in reasonable agreement with that determined from statistical methods (3.4 kpc, CKS; 5.3 kpc, Maciel 1984).

K1-22.—This system has a number of remarkable parallels to K1-14. The discoverer of the PN (Kohoutek 1971) noted that three stars appear near the center of the nebula

and proposed that the brightest of these was the PNN. Smith & Gull (1975) confirmed that this star is very blue, but Kaler & Feibelman (1985) noted that the visual luminosity of the star was too large to match the flux distribution extrapolated from the *IUE* measurements. Instead, Kaler & Feibelman suggested that a fainter object 4″ east of Kohoutek's candidate was the PN's true central star. Our *HST* frames confirm that the original Kohoutek-Smith-Gull star is indeed the PNN, but its visual flux is augmented by a very close visual companion 0.″35 away. In fact, at $V = 17.13$, the companion is so red ($V-I = 1.12$) that it is actually brighter than the PNN in the I band. Given the low stellar density in the field, the pair almost certainly form a bound system. Our derived distance of 1.3 kpc is reasonably consistent with distances based on statistical techniques (1.0 kpc, CKS; 3.4 kpc, Zhang 1995).

K1-27.—The faint companion to K1-27 has the color of a late A star; consequently, if the star is on the main sequence, its faint apparent magnitude ($V \simeq 21.3$) implies an implausibly large distance (55 kpc). There is, however, another possible solution for this system: the companion star could be a white dwarf. Instead of placing the secondary on the main sequence, we obtained the distance given in Table 7 by putting the companion on the white dwarf cooling sequence defined by the hydrogen-rich white dwarf models of Bergeron, Wesemael, & Beauchamp (1995). The locus of points defined by these models is in excellent agreement with that observed for field white dwarfs (Monet et al. 1992), and by adopting the curve, we derive a white dwarf absolute magnitude of $M_V = 12.77$. If we use this value and ignore the nebular Balmer-line extinction estimate $c = 0.28$ (which leads to an unphysically blue color for the central star), then we derive a distance to the system of $\sim$470 pc.

There is only one other distance estimate, statistical or otherwise, for K1-27. By modeling the absorption lines from the hydrogen-deficient central star, Rauch, Köppen, & Werner (1994) derived a distance to the object of $1.29^{+1.05}_{-0.58}$ kpc. This number, however, assumes $c = 0.28$; with a more reasonable value of $c = 0.08$, their distance decreases by a factor of $\sim$1.2 and comes into marginal agreement with ours. In most other respects, our white dwarf hypothesis is reasonable. At an absolute magnitude of $M_V = 12.77$, the cooling age of a 0.575 $M_\odot$ companion white dwarf is $\sim$1 Gyr (cf. Bergeron et al. 1995), and thus the star would not be in a particularly rapid phase of evolution. Similarly, if the distance is indeed 0.47 kpc, then the derived values for the nebular size (0.1 pc) and binary separation (260 AU) are also plausible. The only potential problem lies in the extremely small amount of flux radiated by the nebula in [O III] λ5007. At an absolute [O III] λ5007 magnitude of $M_{5007} \sim 8.7$, the nebula would be a full 13.1 mag fainter than the bright end of the [O III] λ5007 planetary nebula luminosity function (Ciardullo et al. 1989; Jacoby et al. 1992), and the intrinsically faintest [O III] λ5007 source in the Strasbourg-ESO planetary nebula catalog (Acker 1992). Note, however, that the nebular and central-star properties of K1-27 (Henize & Fairall 1981; Méndez, Kudritzki, & Simon 1985) are very similar to those of Abell 36, an extremely high excitation object which, from its [O III] line flux and statistical distance, *is* the faintest [O III] λ5007 source currently in the catalog ($M_{5007} \sim 7.2$). In fact, both Henize & Fairall and Méndez et al. have remarked that the properties of the K1-27 nebula and central star are more extreme than those of Abell 36, and a large fraction of the nebula's oxygen is in O IV. Consequently, the intrinsically small amount of [O III] λ5007 emission is entirely reasonable. We consider this a likely white dwarf-PNN binary system.

Mz 2.—This PN is 3° from the Galactic plane and only 31° from the Galactic center. Thus, the field star density in the region is extremely high: there are over 3400 stars recorded on our WF/PC frames. Nevertheless, only five of these stars are as bright as, or brighter than, our putative companion. The relative scarcity of $I = 15.8$ stars, and the small (0.″28) separation between the PNN and the companion, leads to a very high probability (99.99%) of a physical association.

Our distance to Mz 2 of $\sim$2.2 kpc is in good agreement with most statistical distance estimates (2.3 kpc, CKS; 2.4 kpc, Van de Steene & Zijlstra 1994; 2.7 kpc, Zhang 1995). Kingsburgh & English (1992) derive a somewhat larger distance ($\sim$5 kpc) from the PN's location on the [O II] density-ionized mass relation, but the subsequent classification of the object as a type I PN (Perinotto et al. 1994) vitiates this analysis.

NGC 1535.—The companion to this well-studied PNN has the colors of an early G star. If the pair forms a bound system, then the projected separation between the two stars is $\sim$2400 AU and the distance to the binary is $\sim$2.3 kpc. This value is in excellent agreement not only with most modern statistical distances (2.3 kpc, CKS; 2.0 kpc, Van de Steene & Zijlstra 1994; 2.1 kpc, Zhang 1995) but with the distance derived from the non-LTE model-atmosphere analysis of its central star (2.0 kpc, Méndez, Kudritzki, & Herrero 1992). This consistency, along with the small probability of a chance superposition, supports the interpretation that this is a true physical system.

NGC 3132.—The binary nature of this PNN was first discovered by Kohoutek & Laustsen (1977). The companion star has an A0 V spectral type (Lutz 1977), which implies that the PN was ejected from an even more massive progenitor. The hot star, which is only marginally resolved from the ground, is easily measured on our PC frame and is 5.65 mag fainter in V than its companion; if we place the A star on the main sequence, we obtain a distance to the system of $\sim$0.8 kpc. This is consistent with estimates based on the interstellar reddening along the line of sight (Gathier, Pottasch, & Pel 1986) and the ground-based spectroscopic parallax of the A star (Pottasch 1980).

Unfortunately, there are two caveats that accompany our distance measurement. The first arises out of the definition of our field star main sequence. For a PN to exist, the age of the system must be at least $\sim 5 \times 10^7$ yr (Bressan et al. 1993); this is a nonnegligible fraction of the main-sequence lifetime of the A star. Consequently, some main-sequence evolution must have occurred, and the companion could be up to $\sim$0.2 mag brighter than its zero-age main-sequence luminosity. While the effect is partially mitigated by our use of a field star main sequence rather than a zero-age main sequence, it is still likely that the companion is older than a typical A-type field star. Fortunately, the effect is small: the difference between the expected mean magnitude of a group of A stars of all ages, and that of a sample of stars with ages of at least $\sim 5 \times 10^7$ yr, is only $\sim$0.05 mag.

The second problem comes from the uncertainty in our reddening estimation. On the lower main sequence, the V versus $V-I$ reddening vector is roughly parallel to the main sequence. Consequently, a small error in the extinc-

tion makes little difference to a distance derivation: both V_0 and M_V are modified in a similar fashion. For A stars, however, this is not the case, as the slope of the main sequence is significantly steeper. The result is that a small uncertainty in reddening translates into a large uncertainty in distance. In the case of NGC 3132, the uncertainty in our color-based reddening estimate, $\sigma_{E(V-I)} \sim 0.11$ mag, translates into a ~ 0.64 mag uncertainty in distance modulus. This dominates the error given in Table 7. Strömgren photometry of the A star would improve the distance estimate considerably.

NGC 7008.—It is somewhat surprising that the composite nature of the nucleus of NGC 7008 was not detected prior to our survey. Although the angular separation between the PNN and the companion is small (0.″4), the magnitude difference between the two stars is only ~ 0.5 mag in V, and in I the light from the companion star actually dominates. By placing the companion on the main sequence, we obtain a distance of ~ 0.4 kpc, and an implied stellar separation of ~ 160 AU. This compares with a distance of ~ 1.1 kpc estimated from extinction measurements along the line of sight (Pottasch 1983), and the CKS statistical distance of ~ 0.9 kpc. Because the probability of a chance superposition of a $V \sim 14$ mag star near the PNN is extremely small, we consider this a good binary star candidate.

There is one caveat to our distance, however. On both of our F814W frames, the point-spread function for NGC 7008's companion star appears slightly broader than expected from a normal single star. The effect is not large, and we cannot rule out the existence of an instrumental problem. However, it is possible that the companion is itself a binary, making the PNN a hierarchical triple. If this is the case, our distance to the object is an overestimate.

Sp 3.—The companion in this system has the color of an F-type star and is only 0.″3 from the PNN; when we place it on the main sequence, we derive a distance of ~ 2.4 kpc, in good agreement with the CKS statistical distance of 1.9 kpc. This consistency, along with the small probability of superposition, indicates that this is a true physical association.

6.2. *Possible Physical Pairs*

Abell 7: Our 200 s I-band Planetary Camera image shows only two stars on the frame: the PNN and a very faint companion only 0.″9 away. Since the stellar density in this field is low (it is at $b = -30°$), there is a very high probability that the stars are physically associated. Unfortunately, the companion is ~ 5.3 mag fainter than the central star in I and so red that it was not detected on our V frames. This implies a $V-I$ color redder than 1.21 and an absolute magnitude fainter than $M_V = 6.7$.

From main-sequence fitting, we can derive only an upper limit to Abell 7's distance of ~ 13 kpc. This limit is not particularly useful, as the size of the nebula (760″) and the central star's white dwarf spectrum (Liebert 1980) demand that the object be quite nearby. If the CKS statistical distance of ~ 200 pc is accurate, then the projected separation between the PNN and the companion star is only ~ 200 AU. Deeper images are desirable to investigate this interesting object further. In the meantime we can only classify A7 as a possible physical binary.

Abell 30.—The companion to Abell 30 was found from the ground by Cudworth (1973). The position angle has not changed significantly over the ensuing ~ 25 yr, and our main-sequence fitting distance (~ 2 kpc) is consistent with the CKS statistical distance of 1.7 kpc. On the other hand, the relatively large separation (5.″25) does allow a $\sim 2\%$ probability of a chance superposition. Moreover, at a distance of 2 kpc, the derived physical separation of the pair ($\sim 10{,}600$ AU) is starting to approach the observed 0.1 pc cutoff imposed by the Galactic tidal field (cf. Bahcall & Soneira 1981; Latham et al. 1984). We therefore categorize A30 only as a "possible" physical association.

Abell 63.—The central star of Abell 63 is the 11 hour eclipsing binary UU Sge (Bond, Liller, & Mannery 1978); the PNN's nearby companion (2.″8 away) was first noted during photoelectric observations by Krzeminski (1976). In spite of the PN's low galactic latitude, $b = -3°$, we find only a 1.5% probability that the resolved companion is a chance superposition. Based on the nebular Balmer decrement, the extinction to the object is $c = 0.71 \pm 0.10$ (Walton, Walsh, & Pottasch 1993); this number is in excellent agreement with the value obtained by modeling the 2200 Å interstellar absorption feature (Walton et al. 1993; Pollacco & Bell 1993). When we combine this extinction estimate with our *HST* photometry, we derive a distance to the companion star of ~ 1.2 kpc.

From the run of stellar reddening versus distance in that part of the sky, a foreground extinction of $c \sim 0.7$ [$E(B-V) = 0.5$] implies a distance of ~ 1 kpc (cf. Bond et al. 1978), in good agreement with our findings. However, analyses of the spectral type and color of the back hemisphere of the extremely close eclipsing companion yield values that are 2–3 times larger (~ 3.6 kpc, Walton et al. 1993; 3.2 ± 0.6 kpc, Pollacco & Bell 1993; 2.4 ± 0.4 kpc, Bell, Pollacco, & Hilditch 1994). These distances could be overestimates if some of the extreme heating effects on the companion "leak" around to the unilluminated back side. Unfortunately, without improved observations, we can only identify this as a possible physical system.

IC 4637.—This new pair—which, remarkably, was never noted from the ground—was discovered on our original Cycle 3 F785LP WF/PC frame and followed up with WFPC2 (F555W and F814W) observations. The implied separation between the PNN and its companion, ~ 1200 AU, is large, but not excluded by any means; similarly, the derived nebular size of ~ 0.05 pc is small, but again, not unreasonable. Interestingly, the statistical distances to this object vary widely, from 0.8 kpc (Amnuel et al. 1984) to 2.3 kpc (CKS), but all estimates lie on the high side of our 0.5 kpc value. Furthermore, the object's only individual distance determination, the non-LTE model atmosphere value of Méndez, Kudritzki, & Herrero (1992), is larger still (3.3 kpc). We are therefore led to classify this object only as a possible physical binary.

NGC 2392.—Like Abell 7, NGC 2392 has a faint companion, which is barely detected on our I frames and is invisible in V. Our upper limit to the distance, ~ 6.4 kpc, is not particularly useful, since both non-LTE model atmospheres (Méndez et al. 1992) and statistical techniques (CKS; Van de Steene & Zijlstra 1994; Zhang 1995) place the object closer than ~ 2 kpc. Deeper imaging could provide a photometric distance, but for the present, the lack of a V magnitude forces us to categorize the object as a "possible" physical association.

NGC 2610.—Again, there is a close (0.″6), extremely faint companion to this object that could not be detected on our V images. A much deeper image is needed to produce a

meaningful distance estimate. We again categorize this as a "possible" physical system.

6.3. *Doubtful Physical Pairs*

Abell 24.—The visual companion to this star was first noted by Cudworth (1973). We measure a separation of 3.″33, in good agreement with the 3.″4 reported by Cudworth. However, our measurement for the position angle of the binary differs by 5° from his value; this offset marginally exceeds the uncertainty in the old measurement (K. M. Cudworth 1997, private communication). Since for any plausible distance, this change in position angle is larger than is possible from binary orbital motion, the difference argues against the existence of a physical association. Other facts suggestive of a chance superposition include the extremely large diameter derived for the nebula ($\sim$4 pc) and the factor of 5 difference between our putative distance ($\sim$2.4 kpc) and distances derived from statistical techniques (e.g., 0.52 kpc; CKS). Despite the fact that the formal probability of a chance superposition is only $\sim$2%, we believe that this object is an optical double.

NGC 650-1.—The companion star of this object was first noticed by Cudworth (1973). However, our *HST* images reveal that the companion is itself a very close double, with a separation of only 0.″16. Given the field star density of the region, the two stars of the companion almost certainly form a physical system, as the probability of a 0.″16 chance superposition is less than 0.1%. However, associating the companion binary with the PNN is more problematic.

The separation and position angle of the companion pair relative to the PNN is the same as it was 25 yr ago; thus, despite the fact that the probability of a chance association is $\sim$5%, this may argue for a physical association. However, if the system is a hierarchical triple, then it is a very peculiar one: although both components of the companion have the same color, $(V-I)_0 \approx 0.87$, one is 0.8 mag brighter than the other. In other words, both stars cannot be on the main sequence. If the PNN is associated with this pair, then two of the three stars of this noninteracting trinary happen to be in a phase of rapid evolution.

The hypothesis of a bound triple system runs into further problems when one considers the age and metallicity of the stars. NGC 650-1 is a metal-rich type I planetary nebula, with a most likely progenitor mass $M \gtrsim 2\,M_\odot$ (Peimbert & Torres-Peimbert 1983). Yet if we assume a solar-like metallicity and place the fainter component of the close pair on the main sequence, then the position of the brighter component in the color-magnitude diagram demands that the system be impossibly old. As the isochrones in Figure 6 show, both of the close components could lie on or close to the same isochrone if the $V-I$ colors were near the blue ends of their error bars, but the age of the pair would still be far in excess of that of the PNN. A lower age for the close pair would be possible if a substantial amount of additional reddening were adopted. However, if that were the case, then the reddening would greatly exceed that of the PNN itself, and we would be forced to conclude that the two systems were unrelated. Another alternative is that the fainter component of the close pair is on the main sequence, and the brighter component is itself an unresolved binary containing two equal-brightness main-sequence stars; although not impossible, this option would imply the unlikely conclusion that the close pair is actually a hierarchical triple containing three stars of essentially identical mass.

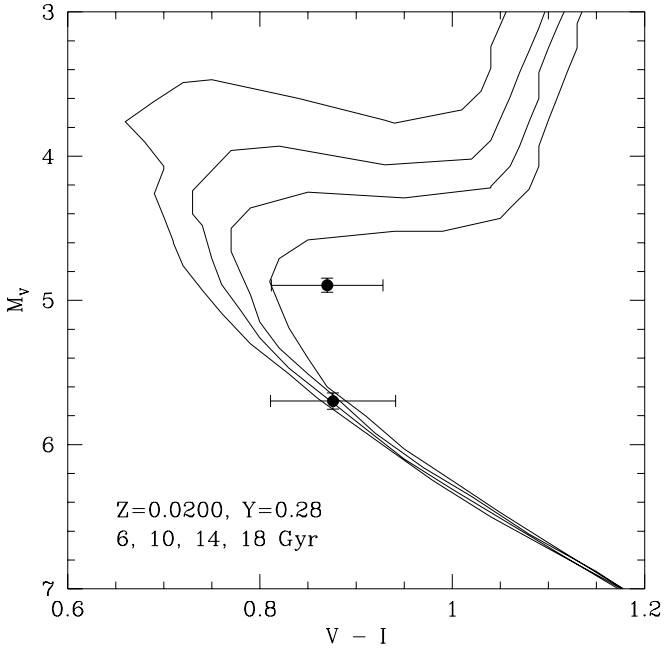

FIG. 6.—Positions of the two companion stars to the nucleus of NGC 650-1 in the HR diagram under the assumption that the fainter star is on the main sequence. Superposed for comparison are the 6, 10, 14, and 18 Gyr solar metallicity isochrones from Bertelli et al. (1994). The error bars reflect photometric uncertainties only and do not include the contribution of the uncertain foreground reddening. As discussed in the text, since NGC650-1 likely comes from a massive progenitor, it seems probable that the PNN and the companions are not associated.

The distance of 4.1 kpc given in Table 7 was derived by fitting the fainter component of the close pair to the main sequence; it exceeds the statistical distances (CKS: 0.7 kpc; Zhang 1995: 1.6 kpc; Van de Steene & Zijlstra 1994: 1.3 kpc) by a substantial amount. We therefore suspect that the very close pair, whatever its astrophysical explanation, is probably significantly more distant than—and older than—the PNN and thus not physically associated.

PuWe 1.—A slightly brighter companion to the central star of this object is visible on the Palomar Sky Survey at a separation of 5″ (Purgathofer & Weinberger 1980), but our WF/PC observations reveal that the companion is itself resolved into two stars with a separation of 0.″6. Unlike the NGC 650-1 system, both cool components are apparently on the main sequence, as they produce a consistent set of distances. Since the PN is an extremely large object that extends over 10′ on the sky (Purgathofer & Weinberger 1980), we expect it to be relatively nearby, and our derived distance of $\sim$280 pc does not contradict this hypothesis.

Nevertheless, the PuWe 1 PNN is probably not associated with the close pair. Based on the stellar density in the region, and the rather large (5″) separation between the PNN and the companions, the likelihood of a chance superposition in the region is relatively large, $\sim$3%. Moreover, PuWe 1 is one of the few PNNs with a reliable trigonometric parallax measurement, 2.3 ± 0.4 mas (Harris et al. 1997). This is more than 2 σ smaller than we would predict based on our companion star measurements. Even more telling is that the proper motion of the close pair appears to be significantly different from that of the PNN (H. C. Harris 1998, private c communication). Thus, we believe the stars are not physically associated.

6.4. *Noteworthy Optical Doubles and Unresolved Objects*

Several other stars in our survey were included because they were identified as candidate visual binaries on the basis of ground-based observations, but we have concluded that they are not physical pairs. In addition, a few other objects are definitely binaries, based on their composite spectra and/or red colors, but we did not resolve them. These objects are discussed in this subsection.

Abell 78.—In his survey of the nebular features of this PN, Jacoby (1979) noted that an extended patch of Hα emission $\sim 10\farcs2$ from the PNN was spatially coincident with a star, but that there was no other evidence for a physical association. Our star counts in the region suggest that the "companion" is most likely an unrelated field star that is merely projected onto the nebula.

Abell 82.—A82 has a diameter of about 90″ and was included in our program as a candidate binary because, as recounted by Kaler & Feibelman (1985), there is a relatively bright late-type star at the center of the nebula. Kaler & Feibelman's *IUE* spectra did reveal a weak, apparently reddened, UV continuum within the 10″ × 20″ aperture of the instrument, but the derived color temperature was much too low to explain the nebula's ionization. The central object has a K-type spectrum (Kaler & Feibelman 1985) and colors of $V = 14.90$, $B-V = 1.28$, and $V-I = 1.36$ (Kwitter, Jacoby, & Lydon 1988 and our *HST* measurements). Kwitter et al. have suggested that the image of the K star masks the true PNN on ground-based photographs (cf. the case of K1-14 above), but we find no evidence on our *HST* frames for any blue object near the center of the nebula. Alternatively, Kaler & Feibelman (1985) have proposed that a faint object 6″ northwest of the K star is the PNN, but our photometry ($V = 18.15$, $V-I = 1.10$) demonstrates that this star is not blue either. In fact, the bluest object on our PC frame is a $V = 12.85$, $V-I = 0.35$ star located 18″ southeast of the K star. This star might have been within the *IUE* aperture if the pointing was slightly inaccurate and thus could be the reddened source detected by Kaler & Feibelman. However, it is too far off-center to be the planetary's central star.

In view of the above ambiguities, we investigated the *IUE* observations in further detail, with the aid of copies of the original observing scripts which were kindly provided by W. A. Feibelman. Two short-wavelength spectra were obtained, SWP 19771 (1983 Apr 20; 25 minutes), which shows no convincing detection, and SWP 19908 (1983 May 5; 120 minutes), which detected the reddened continuum described above and shows that the source was well centered in the aperture. For both observations, a blind offset was done from a nearby 11th magnitude star onto the coordinates of the center of the PN. Our measurements on the Digitized Sky Survey show that the resulting pointing would have been about 10″ directly west of the 14th magnitude K-type star and thus would either have missed it or at best have had it at the edge of the aperture. However, handwritten notes from the telescope operator indicate that a possible additional telescope movement may have been performed onto a "second central star," which we speculate could have been the 12.8 mag star to the southeast of the K star. In this case, the weak UV spectrum would be nicely explained. If so, however, it appears that *IUE* never actually observed the star at the center of the PN.

We are thus left with two plausible conclusions: either the true hot central star is a faint, unresolved companion of the K-type star; or a born-again scenario (see next paragraph) for the K star itself may have to be invoked. Further ground- and space-based spectroscopic observations of this PNN are urged.

He 1-5 and *H3-75.*—The central star of He 1-5 is the well-known object FG Sge, which appears to be a PNN that has undergone a late helium thermal pulse and has become a born-again red giant. In agreement with spectroscopic observers (e.g., Feibelman & Bruhweiler 1990) and in agreement with the born-again scenario, we find no evidence for a hot companion in our *HST* images. H3-75 is an interesting and possibly related object: according to N. Sanduleak (1984, private communication), the central star has a K-type spectrum. *IUE* ultraviolet spectra (Bond 1993) show no trace of a hot star, and our *HST* frames likewise show no resolved companion. The PNN is therefore a strong candidate for another born-again giant. Spectroscopic observations are needed.

He 2-36.—The optical central star of He 2-36 has a spectral type of A2 III (Méndez 1978), and *IUE* observations suggest the presence of a hot companion (Feibelman 1985). Our frames do not resolve the binary.

M1-2.—This object has a G2 Ib spectral type (O'Dell 1966) and strong forbidden and permitted emission lines reminiscent of those seen in a planetary nebula (see Grauer & Bond 1981 and references therein). Our *HST* observations do not resolve any binary companion, nor do they show a resolved nebular component. The system is probably a symbiotic-like binary that is too compact to be resolved by *HST*, although Feibelman (1983) has argued from *IUE* observations that the star is surrounded by a young planetary nebula.

NGC 1514.—The central star is a well-known composite system, containing a hot sdO star and an A-type companion (Kohoutek & Hekela 1967; Greenstein 1972). Greenstein's radial velocity measurements indicate that the period of the system must be quite long (or perhaps that the binary is seen nearly pole-on). Nevertheless, our *HST* images fail to resolve the system, setting an upper limit of approximately 40 AU for the projected separation.

NGC 6853.—The binarity of the PNN was first suggested by Cudworth (1973), who identified a $V \simeq 17$ companion $6\farcs5$ from the central star. Astrometric measurements (Cudworth 1977) support this contention, as the proper motion of the companion is similar to that of the central star. Unfortunately, given the density of field stars in the region, our probability calculations cannot confirm this claim of binarity, as there is almost a 90% chance that a random field star will be projected within $6\farcs5$ of the PNN. In fact, based on the star counts, the best candidate for association with NGC 6853 is a $V \approx 18.7$ star $1\farcs1$ from the central star, but even this object has a 12% probability of being a chance superposition. We do note that if we assume Cudworth's star is associated with the PNN, then our *HST* photometric values of $V = 16.91$, $V - I = 1.83$, coupled with the assumption of no foreground reddening, leads to a distance of 430 ± 62 pc. This is in agreement with the distance of 380 ± 64 pc recently obtain by Harris et al. (1997) from USNO parallax measurements. In keeping with the precepts of this paper, we will not discuss this object any further, but we urge radial velocity measurements for the system.

Th 2-A.—As noted in § 2, this object was included in our

program because of a nearby companion noted on ground-based CCD frames. However, there are over 2300 field stars present on our *HST* frames, and the star in question has a $\sim 50\%$ probability of being a chance superposition. We therefore cannot classify it as a possible visual binary.

A34 and A66.—Like Th 2-A, nearby companions were noted during ground-based observations. The companion of A34 has a 28% probability of being there by chance, and for A66 the probability is 21%.

A46, *A65*, *HFG 1*, *K1-2*, *LoTr 5*, and *NGC 2346.*—All of these central stars (along with A63, discussed above) are known to be extremely close binaries, based on their photometric variability (cf. Bond & Livio 1990). Not unexpectedly, none of them were resolved in our survey, and we do not find any nearby resolved companions that have a high probability of being physically associated.

7. COMPARISON WITH STATISTICAL DISTANCE SCALES

Because of their complexity and vast range in size, luminosity, mass, and excitation, there is no reliable method for obtaining distances to large samples of individual Galactic planetary nebulae. As a result, in order to investigate planetary nebulae as a class, it is necessary to rely on statistical distance estimators. The principle behind these statistical distances is straightforward: the emitted Balmer-line flux from an ionized plasma depends almost exclusively on the total mass of the emitting region and the plasma density. Consequently, if the ionized mass of a nebula can be estimated, then its observed flux and angular size can be used to calculate its distance. The key, of course, is to know the amount of ionized mass contained in the nebula.

There are several prescriptions in the literature for estimating this mass, starting with the original assumption by Shklovsky (1956) that the ionized masses of all PNe are the same and that all PNe are optically thin. Other formulations include adopting an ionized mass that is (1) linearly proportional to nebular radius (Maciel & Pottasch 1980), (2) proportional to a power of the radius (Zhang 1995), (3) proportional to the radio brightness temperature of the nebula (Van de Steene & Zijlstra 1995, hereafter VdSZ), (4) dependent on the [O II]-derived nebular density (Kingsburgh & Barlow 1992; Kingsburgh & English 1992), or (5) constant for optically thin nebulae but proportional to an optical-thickness parameter for denser objects (Daub 1982; CKS). Once calibrated, each of these relations is capable of producing distance estimates to large numbers of objects.

Unfortunately, the number of PNe with independently known distances, which can therefore be used as zero-point calibrators for these methods, is extremely small. Moreover, some of the calibrators have distances that are themselves controversial. For example, CKS used 19 PNe with "well-determined" distances to calibrate their distance scale, while VdSZ used 23 calibrators. A comparison of the two samples, however, reveals that only 16 PNe are common to both data sets, and of those, two objects have adopted distances that differ by more than a factor of 2! A major reason for this dichotomy is that many of the well-determined PN distances are based on such methods as reddening of field stars projected near the PN line of sight (Gathier, Pottasch, & Pel 1986), Galactic H I absorption measurements (Gathier, Pottasch, & Goss 1986), nebular expansion parallaxes (e.g., Hajian et al. 1995), and non-LTE atmospheric modeling of PN central stars (e.g., Méndez et al. 1992). None of these methods is unassailable, and each carries its own (possibly substantial) uncertainty.

Our new sample of PNe with visual-binary nuclei significantly increases the number of objects with reliable distance measurements and constitutes a new and important set of data with which to calibrate PN statistical distances. In addition to having quantifiable errors, the PNe in our sample have distinctly different selection criteria from those measured by other methods. PNe with ISM-based distances are mostly distant objects in the plane of the Milky Way. Similarly, PNe with nebula-expansion distances are objects that are bright and optically thick, while those analyzed with non-LTE model atmospheres have highly evolved central stars. Our wide binary stars, however, are primarily nearby objects and objects at high galactic latitude. Consequently, our sample not only enlarges the PN calibrator database but also reduces the possibility of a systematic error due to selection biases.

The usefulness of our data set for testing statistical distance techniques is demonstrated in Figure 7, which compares directly measured PN distances with those from four different statistical methods. For the directly measured distances, we use the 10 "probable" associations listed in Table 7 (one of which, A31, is only an upper limit), along with the three additional distances to the "possible" associations that are not upper limits. To these we add the new ground-based distance to NGC 246 (based on photometry of its wide binary companion; Bond & Ciardullo 1999) and trigonometric distances to seven PNe derived from recent parallaxes greater than 3 σ measured by the *Hipparcos* satellite (ESA 1997) and the US Naval Observatory (Harris et al. 1997).

These accurate photometric and geometrical distances are plotted against statistical distances computed from the 5 GHz flux measurements and angular diameters given by Zhang & Kwok (1993) and CKS, using the prescriptions of CKS, VdSZ, Maciel & Pottasch (1980), and Zhang (1995). For reference, the data of Figure 7 are given in Table 8.

It is immediately obvious that distances from all of the statistical methods have considerable dispersion. Compared with the binary and astrometric distances, the CKS and Zhang estimates scatter by $\sigma \sim 1.7$ mag and $\sigma \sim 1.8$ mag in distance modulus, respectively. The VdSZ distances exhibit the smallest dispersion, ~ 1.6 mag, while the Maciel estimates have the largest, ~ 2.4 mag. (This last result is not very surprising, since some of the PNe considered here have radii outside the formal limits of the Maciel calibration.) Interestingly, a significant amount of dispersion is attributable to one object, PHL 932, which has a *Hipparcos* parallax distance of 110^{+48}_{-26} pc but statistical distances that range from 800 pc (CKS) to 5.0 kpc (Zhang). The central star of PHL 932 is an exceptionally unusual object. With a sdB spectral type (Méndez et al. 1988), it is one of only two known PNNs of this class, lying well off the normal post-AGB evolutionary tracks. It has been suggested that the star may have evolved through a common envelope binary interaction (Iben & Tutukov 1993), and thus the ionized mass could differ substantially from that of normal PNe. If PHL 932 is arbitrarily disregarded, then the dispersion in the VdSZ and Zhang errors drops dramatically to ~ 1.1 and ~ 1.3 mag, respectively. Even this, however, is much larger than the errors expected from the techniques.

Even more surprising are the zero-point offsets in the scales exhibited in the figure. All four of the statistical

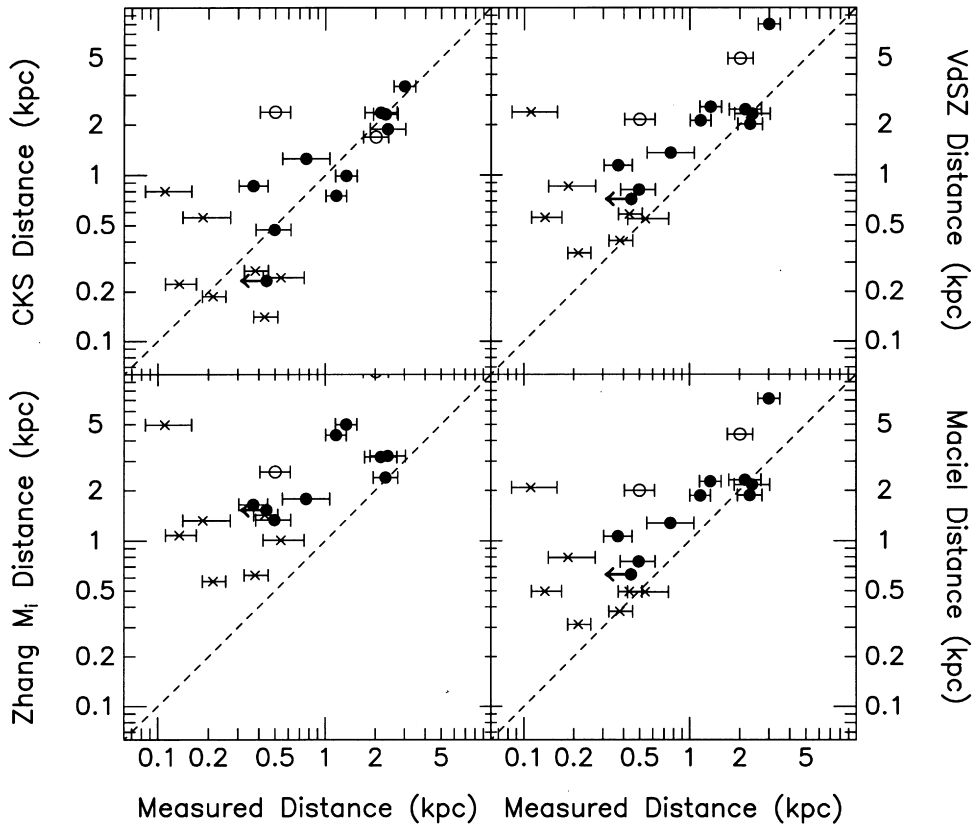

FIG. 7.—Comparison of directly measured distances to planetary nebulae with those from four different statistical methods. Distances from resolved binaries are shown as filled circles, and those from recent PNN parallax measurements are shown as crosses. The open circles show A30 and IC 4637, which are only possible binary associations. Our upper limit of 0.44 kpc for A31 from its resolved companion is shown as an arrow facing left. All four statistical methods systematically overestimate the distances to the PNe in our sample, although for the Cahn et al. (1992) method the overestimate is by only 1 σ.

TABLE 8

STATISTICAL VERSUS MEASURED DISTANCES

NAME	RADIUS (arcsec)	F(5 GHz) dv (Jy)	STATISTICAL DISTANCES (kpc) CKS	VdSZ	Maciel	Zhang	MEASURED DISTANCE (kpc)
Measured from resolved companion:							
A30	63.5	0.0023	1.69	4.97	4.37	10.38	2.02
A31	486.0	0.1019	0.23	0.72	0.63	1.53	0.44
A33	134.0	0.0140	0.75	2.11	1.86	4.32	1.16
A63	...	...	...	...	...	...	1.22
IC 4637	9.3	0.1325	2.37	2.14	2.00	2.59	0.50
K1-14	23.5	0.0014	3.38	7.97	7.15	15.00	3.00
K1-22	90.5	0.0115	0.99	2.55	2.26	4.99	1.33
K1-27	...	...	...	...	...	...	0.47
Mz 2	11.4	0.0750	2.35	2.46	2.31	3.18	2.16
NGC 246	112.0	0.2480	0.47	0.81	0.75	1.33	0.49
NGC 1535	9.2	0.160	2.30	2.01	1.87	2.39	2.31
NGC 3132	22.5	0.230	1.25	1.35	1.27	1.78	0.77
NGC 7008	42.8	0.217	0.86	1.14	1.06	1.65	0.37
Sp 3	17.8	0.0610	1.88	2.31	2.16	3.23	2.38
Measured from trigonometric parallax:							
A21	307.5	0.3270	0.24	0.55	0.49	1.01	0.54
A35	386.0	0.255	0.22	0.56	0.50	1.08	0.13
NGC 1514	80.0	0.288	0.56	0.86	0.79	1.32	0.18
NGC 6853	165.0	1.3249	0.27	0.40	0.37	0.62	0.38
NGC 7293	300.0	1.2919	0.19	0.34	0.31	0.57	0.21
PHL 932	135.0	0.0100	0.80	2.37	2.08	4.97	0.11
PuWe 1	1200.0	0.0847	0.14	0.58	0.49	1.43	0.43

methods examined here systematically overestimate the distances to the objects in our sample. CKS come closest to reproducing our distance scale, with estimates that are, on average, only ~25% larger than the photometric and geometrical measurements. Since this is a 1 σ result, their analysis is still consistent with our measurements. The distance scales defined by VdSZ, Maciel, and Zhang, however, are all significantly too long, with mean distance moduli that are 1.6, 1.2, and 2.7 mag larger than our own. The sizes of these offsets are extraordinary, especially when one considers that the VdSZ and Zhang relations work well for samples of PNe in the Galactic bulge.

Another way of looking at the problem is to compare the properties of our PNe with those of other PNe with "well-determined" distances. Following VdSZ, we plot in Figure 8 the distance-independent PN radio brightness temperature (which is related to the CKS optical depth parameter), against the distance-dependent quantity of PN radius. The filled circles represent planetary nebulae with resolved binary companions, the crosses show PNe with trigonometric-parallax distances, and the open circles are the VdSZ sample of PNe with what they considered to be "well-determined" distances. It is clear from the figure that the PNe in our new sample do not obey the rather tight relation defined by the VdSZ calibrators; at a given radius, the binary and astrometric PNe are systematically fainter in the radio and have a larger amount of scatter (although the scatter is dominated by a few outliers).

We interpret Figure 8 as revealing a classical selection effect. The distances for the PNe in the VdSZ sample come almost exclusively from reddening and H I absorption distance determinations; hence these objects are nearly all relatively bright, high surface brightness PNe that can be seen at great distances along the plane of the Milky Way. Consequently, a calibration using this sample of objects nicely recovers the distances to Galactic bulge PNe. The PNe in our sample, however, are primarily nearby, faint, and optically thin. They represent a population of objects that has apparently received little weight in the calibration of statistical distances.

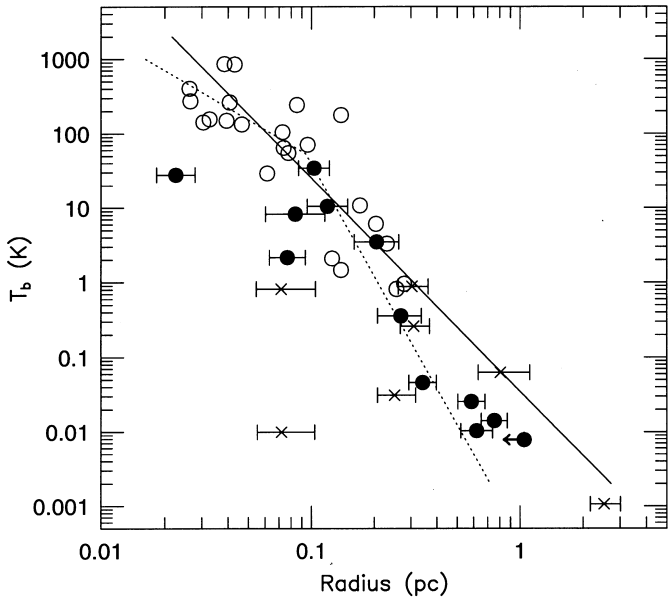

FIG. 8.—Plot of radio brightness temperature determined from 6 cm observations, against derived PN radius for three samples of planetary nebulae. Filled circles represent PNe with visual binary companions, crosses show PNe with trigonometric parallax measurements, and open circles show PNe with distances from Galactic extinction and H I absorption measurements. The solid line is the calibration relation for the Van de Steene & Zijlstra (1995) statistical distance scale; the dotted line with two segments is that for the statistical distance scale of Cahn, Kaler, & Stanghellini (1992). Note that while PNe with ISM-based distances obey the statistical relations, the binary and astrometric PNe have systematically fainter brightness temperatures and a much larger amount of scatter. The data suggest that previous statistical distance scales have been affected by selection effects in the calibration data set and do not work well for low surface brightness nebulae.

Figure 8 also points out the probable cause of a long-standing controversy about the Galactic PN distance scale. For years, there have been two distance scales for Milky Way PNe. The traditional "short" distance scale adopted by Cahn & Kaler (1971) is supported by the extinction-distance relation of Pottasch (1984), the Magellanic Cloud observations of CKS and Webster (1969), and the Galactic bulge measurements of Stasińska et al. (1991). All of these methods use bright PNe, similar to those analyzed in the VdSZ study. The opposing "long" distance scale, which is larger by a factor of ~1.5, is supported by statistical parallax measurements (Cudworth 1974), stellar atmosphere models (Méndez et al. 1992), [O II] line-ratio density estimates (Kingsburgh & Barlow 1992; Kingsburgh & English 1992), and number counts of PNe in other galaxies (Peimbert 1990). These techniques study a different sample of PNe and include local, lower surface brightness objects. Based on the results of Figures 7 and 8, it is therefore not surprising that a different distance scale is derived.

It is unfortunately less obvious—and beyond the scope of this paper—how one could devise a new "grand unification" calibration that simultaneously handles both the lower surface brightness objects that prevail among the nearby nebulae and the brighter PNe that dominate samples like those in the Galactic bulge and extragalactic systems. We leave this daunting task to future workers.

8. CONCLUSION

We have successfully used a large-scale *HST* snapshot survey to find 19 resolved companions of central stars in planetary nebulae. We consider 10 of these systems to be probable physical associations, another six to be possible associations, and the remaining three to be doubtful.

By fitting the companions to the main sequence (or in one case the white dwarf cooling sequence), we have derived reliable distances to the PNe. Comparison with various statistical distance estimates reveals that all of the current statistical methods *overestimate* the distances to our sample. A more detailed examination suggests that the well-studied nebulae used as calibrators for statistical methods are biased toward high surface brightness, low Galactic latitude objects. Our sample, on the other hand, contains more objects of lower surface brightness, which may have systematically lower nebular masses. It will be a challenge to future refinements of the statistical methods to include an additional correction for this effect.

The primary source of error in our PN distance measurements from resolved binaries is the unknown metallicities of the companion stars. This uncertainty propagates directly into the definition of the M_V, $V-I$ main sequence used to obtain the absolute magnitudes (and distance moduli) of the stars. Our distances could therefore be improved substan-

tially via abundance analyses of the nebulae and/or stellar atmosphere analyses (or intermediate-band photometry) of the companion stars. In addition, since several candidate companion stars were detected only in *I*, deeper multicolor imaging with *HST* (possibly with the restored NICMOS camera) could add significantly to the list of PNe with direct distance determinations. Finally, in order to confirm our candidate companion stars and identify additional ones, proper-motion and radial velocity measurements are needed.

We thank H. C. Harris for providing a definition of the field star M_V, $V-I$ main sequence and for unpublished information. We would also like to thank G. Jacoby for instructive conversations at the start of this project and on the properties of optically thin and thick nebulae and for his participation as a Co-Investigator on the Cycle 3 portion of the project. S. Torres-Peimbert provided support at a critical moment. This work was supported by STScI grants GO-04308.01-92A and GO-06119.02-94A and NSF NYI grant AST 92-577833.

REFERENCES

Acker, A., Ochsenbein, F., Stenholm, B., Tylenda, R., Marcout, J., & Schohn, C. 1992, Strasbourg-ESO Catalogue of Galactic Planetary Nebulae (Munich: ESO)
Amaral, L. H., Ortiz, R., Lépine, J. R. D., & Maciel, W. J. 1996, MNRAS, 281, 339
Amnuel, P. R., Guseinov, O. H., Novruzova, H. I., & Rustamov, Y. S. 1984, Ap&SS, 107, 19
Bahcall, J. N., & Soneira, R. M. 1981, ApJ, 246, 122
Bell, S. A., Pollacco, D. L., & Hilditch, R. W. 1994, MNRAS, 270, 449
Bergeron, P., Wesemael, F., & Beauchamp, A. 1995, PASP, 107, 1047
Bertelli, G., Bressan, A., Chiosi, C., Fagotto, F., & Nasi, E. 1994, A&AS, 106, 275
Biretta, J., et al. 1996, Wide Field and Planetary Camera 2 Instrument Handbook, (Baltimore: STScI)
Bond, H. E. 1993, in White Dwarfs: Advances in Observation and Theory, ed. M. A. Barstow (Dordrecht: Kluwer), 85
———. 1994, in Interacting Binary Stars, ed. A. W. Shafter (San Francisco: ASP), 179
Bond, H. E., & Ciardullo, R. 1990, in ASP Conf. Ser. 11, Confrontation between Stellar Pulsation and Evolution, ed. C. Cacciari & G. Clementini (San Francisco: ASP), 529
———. 1999, PASP, 111, 217
Bond, H. E., Liller, W., & Mannery, E. J. 1978, ApJ, 223, 252
Bond, H. E., & Livio, M. 1990, ApJ, 355, 568
Bressan, A., Fagotto, F., Bertelli, G., & Chiosi, C. 1993, A&AS, 100, 647
Brocklehurst, M. 1971, MNRAS, 153, 471
Cahn, J. H., & Kaler, J. B. 1971, ApJS, 22, 319
Cahn, J. H., Kaler, J. B., & Stanghellini, L. 1992, A&AS, 94, 399 (CKS)
Cardelli, J. A., Clayton, G. C., & Mathis, J. S. 1989, ApJ, 345, 245
Casertano, S. 1997, in The 1997 *HST* Calibration Workshop with a New Generation of Instruments, ed. S. Casertano, R. Jedrzejewski, C. D. Keyes, & M. Stevens (Baltimore: STScI), 327
Chopinet, M., & Lortet-Zuckermann, M. C. 1976, A&AS, 25, 179
Ciardullo, R., & Bond, H. E. 1996, AJ, 111, 2332
Ciardullo, R., Jacoby, G. H., & Dejonghe, H. B. 1993, ApJ, 414, 454
Ciardullo, R., Jacoby, G. H., Ford, H. C., & Neill, J. D. 1989, ApJ, 339, 53
Cudworth, K. M. 1973, PASP, 85, 401
———. 1974, AJ, 79, 1384
———. 1977, PASP, 89, 139
Dahn, C. C. 1993, in Galactic and Solar System Optical Astrometry, ed. L. V. Morrison & G. F. Gilmore (Cambridge: Cambridge Univ. Press), 55
Dahn, C. C., et al. 1988, AJ, 95, 237
Daub, C. T. 1982, ApJ, 260, 612
Dopita, M. A., et al. 1997, ApJ, 474, 188
Duquennoy, A., & Mayor, M. 1991, A&A, 248, 485
ESA. 1997, The Hipparcos and Tycho Catalogues (ESA SP-1200) (Noordwijk: ESA)
Feibelman, W. A. 1983, ApJ, 275, 628
———. 1985, AJ, 90, 2550
Feibelman, W. A., & Bruhweiler, F. C. 1990, AJ, 100, 1248
Gathier, R., Pottasch, S. R., & Goss, W. M. 1986, A&A, 157, 191
Gathier, R., Pottasch, S. R., & Pel, J. W. 1986, A&A, 157, 171
Grauer, A. D., & Bond, H. E. 1981, PASP, 93, 630
Greenstein, J. L. 1972, ApJ, 173, 367
Hajian, A. R., & Terzian, Y. 1996, PASP, 108, 419
Hajian, A. R., Terzian, Y., & Bignell, C. 1993, AJ, 106, 1965
———. 1995, AJ, 109, 2600
Harris, H. C., Baum, W. A., Hunter, D. A., & Kreidl, T. J. 1991, AJ, 101, 677
Harris, H. C., Dahn, C. C., Monet, D. G., & Pier, J. R. 1997, in IAU Symp. 180, Planetary Nebulae, ed. H. J. Habing & H. J. G. L. M. Lamers (Dordrecht: Kluwer), 40
Heap, S. R. 1982, in IAU Symp. 99, Wolf-Rayet Stars: Observations, Physics, Evolution, ed. C. W. H. de Loore & A. J. Willis (Dordrecht: Reidel), 423
Henize, K. G., & Fairall, A. P. 1981, PASP, 93, 435
Holtzman, J. A., Burrows, C. J., Casertano, S., Hester, J. J., Trauger, J. T., Watson, A. M., & Worthey, G. 1995, PASP, 107, 1065
Hunter, D. A., Faber, S. M., Light, R., & Shaya, E. 1992, in Wide Field/Planetary Camera Final Orbital/Science Verification Report, ed. S. M. Faber (Baltimore: STScI)
Iben, I., Jr. 1995, Phys. Rep., 250, 2
Iben, I., Jr., & Tutukov, A. V. 1993, ApJ, 418, 343
Jacoby, G. H. 1979, PASP, 91, 754
———. 1989, ApJ, 339, 39
Jacoby, G. H., et al. 1992, PASP, 104, 599
Jacoby, G. H., & Kaler, J. B. 1989, AJ, 98, 1989
Jaschek, C., & Gómez, A. E. 1998, A&A, 330, 619
Kaler, J. B. 1981, ApJ, 250, L31
———. 1983, ApJ, 271, 188
Kaler, J. B., & Feibelman, W. A. 1985, ApJ, 297, 724
Kaler, J. B., & Lutz, J. H. 1985, PASP, 97, 700
Kaler, J. B., Shaw, R. A., & Kwitter, K. B. 1990, ApJ, 359, 392
Kingsburgh, R. L., & Barlow, M. J. 1992, MNRAS, 257, 317
———. 1994, MNRAS, 271, 257
Kingsburgh, R. L., & English, J. 1992, MNRAS, 259, 635
Kohoutek, L. 1971, A&A, 13, 493
Kohoutek, L., & Hekela, J. 1967, Bull. Astron. Inst. Czechoslovakia, 18, 203
Kohoutek, L., & Laustsen, S. 1977, A&A, 61, 761
Krzeminski, W. 1976, IAU Circ. No. 2974
Kwitter, K. B., Jacoby, G. H., & Lydon, T. J. 1988, AJ, 96, 997
Landolt, A. U. 1983, AJ, 88, 439
———. 1992, AJ, 104, 340
Latham, D. W., Tonry, J., Bahcall, J. N., Soneira, R. M., & Schechter, P. 1984, ApJ, 281, L41
Liebert, J. 1980, ARA&A, 18, 363
Lutz, J. H. 1977, A&A, 60, 93
Maciel, W. J. 1984, A&AS, 55, 253
Maciel, W. J., & Pottasch, S. R. 1980, A&A, 88, 1
Méndez, R. H. 1978, MNRAS, 185, 647
Méndez, R. H., Groth, H. G., Husfeld, D., Kudritzki, R. P., & Herrero, A. 1988, A&A, 197, L25
Méndez, R. H., Kudritzki, R. P., & Herrero, A. 1992, A&A, 260, 329
Méndez, R. H., Kudritzki, R. P., & Simon, K. P. 1985, A&A, 142, 289
Méndez, R. H., Miguel, C. H., Heber, U., & Kudritzki, R. P. 1986, in Hydrogen Deficient Stars and Related Objects, ed. K. Hunger, D. Schönberner, & N. K. Rao (Dordrecht: Reidel), 323
Michell, J. 1767, Phil. Trans. R. Soc. London, 57, 234
Minkowski, R. 1960, Mt. Wilson and Palomar Observatories Annual Report 1959–1960 (Pasadena: Carnegie Inst. Washington), 18
Milne, D. K., & Aller, L. H. 1975, A&A, 38, 183
Monet, D. G., Dahn, C. C., Vrba, F. J., Harris, H. C., Pier, J. R., Luginbuhl, C. B., & Ables, H. D. 1992, AJ, 103, 638
O'Dell, C. R. 1966, ApJ, 145, 487
Peimbert, M. 1990, Rev. Mexicana Astron. Astrophys., 20, 119
Peimbert, M., & Torres-Peimbert, S. 1983, IAU Symp. 103, Planetary Nebulae, ed. D. R. Flower (Dordrecht: Kluwer), 233
Perinotto, M., Purgathofer, A., Pasquali, A., & Patriachi, P. 1994, A&AS, 107, 481
Perryman, M. A. C., et al. 1995, A&A, 304, 69
Pollacco, D. L., & Bell, S. A. 1993, MNRAS, 262, 377
Pottasch, S. R. 1980, A&A, 89, 336
———. 1983, IAU Symp. 103, Planetary Nebulae, ed. D. R. Flower (Dordrecht: Kluwer), 391
———. 1984, Planetary Nebulae (Dordrecht, Reidel)
Purgathofer, A., & Weinberger, R. 1980, A&A, 87, L5
Rauch, T., Köppen, J., & Werner, K. 1994, A&A, 286, 543
Ritchie, C. E., & MacKenty, J. W. 1993, WF/PC Photometric Monitoring Results (Baltimore: STScI)
Ritchie, C. E., & MacKenty, J. W. 1994, WF/PC Photometric Monitoring Results Updates (Baltimore: STScI)
Saha, A., Labhardt, L., Schwengeler, H., Macchetto, F. D., Panagia, N., Sandage, A., & Tammann, G. A. 1994, ApJ, 425, 14
Shklovsky, I. S. 1956, Astron. Zh., 33, 222
Shaw, R. A., & Kaler, J. B. 1985, ApJ, 295, 537
———. 1989, ApJS, 69, 495
Smith, L. F., & Aller, L. H. 1969, ApJ, 157, 1245
Smith, M. G., & Gull, T. R. 1975, A&A, 44, 223
Stasińska, G., Fresneau, A., da Silva Gameiro, G. F., & Acker, A. 1991, A&A, 252, 762
Stetson, P. B. 1987, PASP, 99, 191

Terzian, Y. 1993, in IAU Symp. 155, Planetary Nebulae, ed. R. Weinberger & A. Acker (Dordrecht: Kluwer), 109
———. 1997, in IAU Symp. 180, Planetary Nebulae, ed. H. Habing & H. Lamers (Dordrecht: Kluwer), 29
Tylenda, R., Acker, A., Raytchev, B., Stenholm, B., & Bleizes, F. 1991, A&AS, 89, 77
Van de Steene, G. C., & Zijlstra, A. A. 1994, A&AS, 108, 485
Van de Steene, G. C., & Zijlstra, A. A. 1995, A&A, 293, 541 (VdSZ)
Walton, N. A., Walsh, J. R., & Pottasch, S. R. 1993, A&A, 275, 256
Webster, B. L. 1969, MNRAS, 143, 79
Yungelson, L. R., Tutukov, A. V., & Livio, M. 1993, ApJ, 418, 794
Zhang, C. Y. 1995, ApJS, 98, 659
Zhang, C. Y., & Kwok, S. 1993, ApJS, 88, 137